CHAPTER 4:

EXPRESSION PATTERNS OF *BCL11* GENES IN MICE

4.1 Introduction

4.1.1 Current knowledge of *Bcl11* genes expression patterns

Bcl11a and Bcl11b are transcription factors and dysregulation of either protein has been associated with etiology of disease in both human and mouse. Over-expression of Bcl11a following proviral integration resulted in the development of myeloid leukaemia in mice (Nakamura et al., 2000). This transformation event may be partially mediated by the physical interaction of Bcl11a with BCL6 (Nakamura et al., 2000). In contrast, homozygous deletions and point mutations of murine *Bcl11b* resulted in thymic lymphomas (Wakabayashi et al., 2003a). Chromosomal translocation of *BCL11A* was also shown to be involved in lymphoid malignancies in humans (Satterwhite et al., 2001). Additionally, both Bcl11a and Bcl11b have essential roles in murine lymphocyte development (Liu et al., ; Wakabayashi et al., 2003b). Recently, studies have implicated *BCL11A* in other human diseases. For example, *BCL11A* mutations have been identified in human breast cancers (Wood et al., 2007) and a quantitative trait locus (QTL) influencing F cell production maps to the *BCL11A* locus in human thalassemia patients (Menzel et al., 2007). These reports underline the potential importance of *Bcl11* genes in several tissues in human and mouse, and clearly emphasize the need for further characterization of their function and expression.

To date, several studies have reported the expression patterns of Bcl11a and Bcl11b proteins (Avram et al., 2000; Gunnersen et al., 2002; Leid et al., 2004; Nakamura et al., 2000). These studies provide useful information regarding the expression patterns of *Bcl11* genes. For example, expression of both *Bcl11* genes in mice is detected from 10.5 days post-coitum (dpc) and this expression persists till adulthood. During embryogenesis, *Bcl11a* is expressed in both mouse and rat cortex and may be required for neuronal development and differentiation (Gunnersen et al., 2002). In the adult mouse, *Bcl11a* mRNA is detected in the brain and spleen, and found at lower levels in the heart,

liver, testis and lung (Avram et al., 2000; Nakamura et al., 2000). Expression of *BCL11A* is also detected in human hematopoietic cells such as myeloid precursors, B cells, monocytes and megakaryocytes (Saiki et al., 2000). Expression of Bcl11b is detected in the mouse skin during embryogenesis and in adulthood by immmunohistochemistry, suggesting that *Bcl11b* may play a role in development and/or homeostasis of the skin (Golonzhka et al., 2007).

However, there are several limitations in the previous studies. Firstly, with the exception of the report by Golonzhka *et al.*, the rest of published data were primarily based on RT-PCR studies, northern analyses and RNA anti-sense *in situ* hybridization. Hence these methods are not sensitive enough to detect expression of *Bcl11* genes at a single cell level. Next, in order to obtain spatial expression patterns of genes using adult tissues such as mammary tissues, penetration of *in situ* probes and antibodies becomes extremely difficult. Therefore it is not feasible to use *in situ* hybridization or antibody staining to detect whole mount spatial expression of genes. To overcome these technical limitations and/or difficulties, I chose the bacterial *lacZ* gene as the reporter gene and generated the *Bcl11-lacZ* reporter mice.

4.1.2   Using *E. coli lacZ* as a reporter in mice

The bacterial *lacZ* gene, encoding the enzyme β-galactosidase (β-gal), is a commonly used reporter gene in mouse genetics because β-gal activity can be readily assessed *in vivo*. By targeting *lacZ* to the *Bcl11* loci, the endogenous *Bcl11* regulatory elements would control expression of *lacZ*. Therefore spatial expression patterns of *Bcl11* genes can be easily detected by staining of the embryos and tissues with 5-bromo-4-chloro-3-indolyl-β-D-galactoside (X-gal) to produce a blue product, 5-bromo-4-chloro-indigo. Using this approach, fine-resolution visualization of cell lineage in vertebrate nervous system has been studied (Trainor et al., 1999). In addition, with the *lacZ* reporter mice, expression of the genes can also be detected at a cellular level using Fluorescein di-β-D-galactopyranoside (FDG). FDG is a fluorescent substrate of β-gal and is used in fluorescence activated cell sorting (FACS) analysis to detect β-gal activity in live cells. Therefore, using FDG in combination with other cell surface markers, one can determine the expression of *Bcl11* genes in specific cell types at a single cell level. Furthermore, β-

gal was found to be more effective in providing signal in the context of weak enhancers and to be extremely useful in high-resolution histochemical analysis (Timmons et al., 1997). Hence regions of low levels of *Bcl11* expression can be detected using the *Bcl11-lacZ* reporter mice.

In the first part of this Chapter, I will describe the use of *Bcl11-lacZ* reporter mice to characterize the spatial expression patterns of *Bcl11* genes in both embryonic and adult developmental stages in whole mount X-gal staining. Subsequently, I will describe the dynamic expression patterns of *Bcl11* genes in both the mammary epithelial and hematopoietic cells using FDG staining and flow cytometry.

4.2 Results

4.2.1 X-gal staining patterns faithfully recapitulate endogenous *Bcl11* expression

The X-gal staining patterns of $Bcl11a^{lacZ/+}$ and $Bcl11b^{lacZ/+}$ 10.5-11 dpc heterozygous embryos were first compared to whole mount *in situ* hybridization patterns (using antisense *Bcl11a* and *Bcl11b* RNA probes) obtained from VisiGene (http://genome.ucsc.edu/cgi-bin/hgVisiGene) (Figure 4.1). X-gal staining of $Bcl11a^{lacZ/+}$ and $Bcl11b^{lacZ/+}$ embryos revealed the expression of *Bcl11a* and *Bcl11b* in the forebrain, derivatives of the pharyngeal arches and limbs, which were similar to the RNA *in situ* hybridization patterns. Hence the X-gal staining pattern is a faithful recapitulation of endogenous *Bcl11* expression.
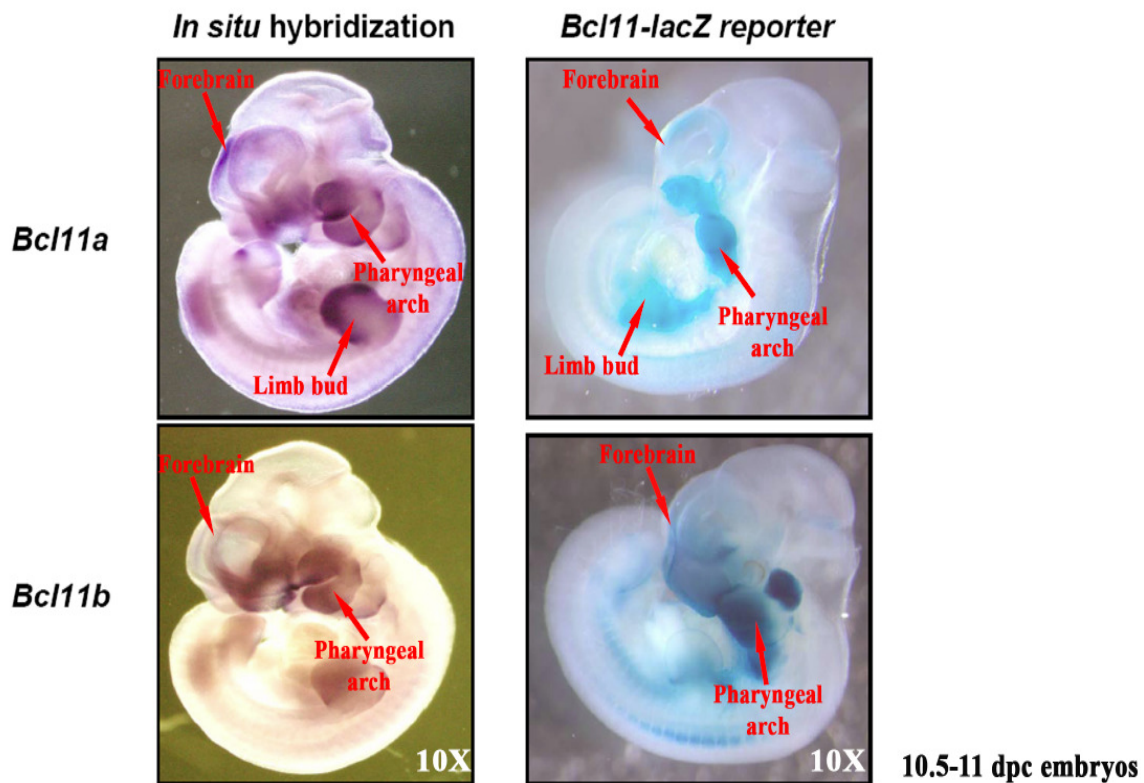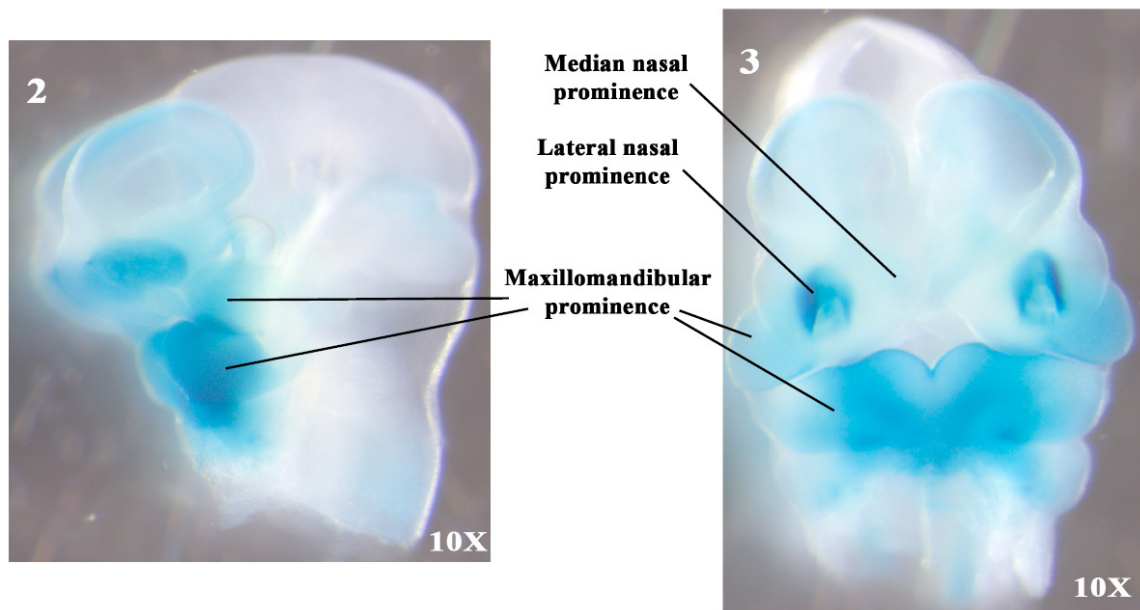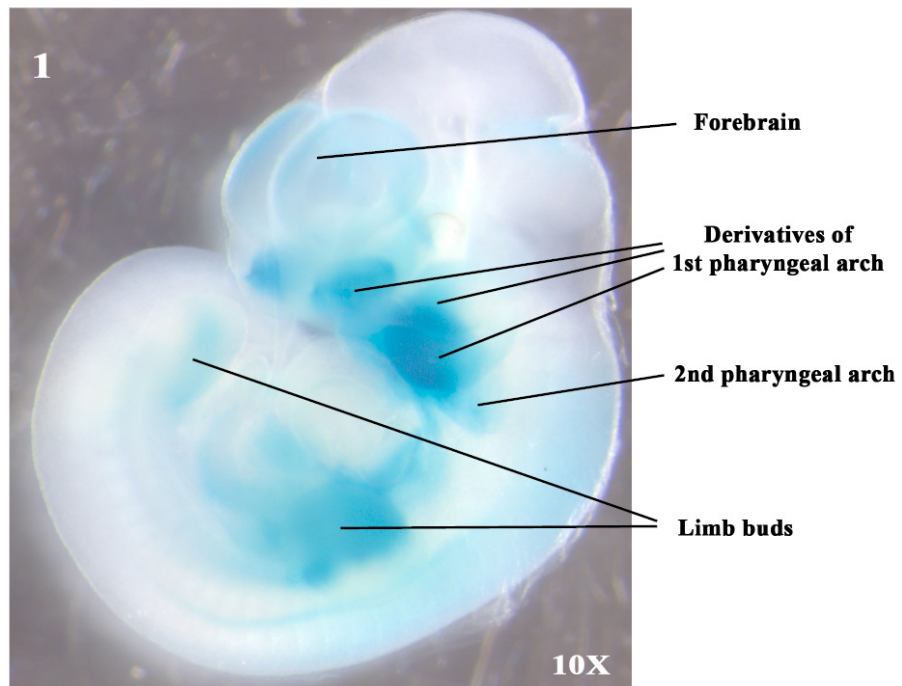

Figure 4.1. Validation of X-gal staining patterns of $Bcl11^{lacZ/+}$ 10.5-11 dpc embryos. Images showing faithful recapitulation of X-gal staining patterns of both $Bcl11a^{lacZ/+}$ and $Bcl11b^{lacZ/+}$ embryos (right panels) as compared to *in situ* hybridization patterns (left panels; images obtained from Visigene).

4.2.2 *Bcl11* genes are expressed in early embryonic development

Expression of *Bcl11a* and *Bcl11b* was first observed at 10.5 dpc, consistent with a previous study (Nakamura et al., 2000). The expression patterns of the two genes partially overlapped at this stage (Figure 4.2A and 4.2B). Both genes were expressed in the forebrain and derivatives of the first and second pharyngeal arches (Figure 4.2A1 and Figure 4.2B1). In addition, high levels of expression of both genes were also detected in the lateral nasal and maxillomandibular prominence and at a lower level in the median nasal prominence (Figure 4.2A2-3 and Figure 4.2B2-3). Several regions of differential expression were also observed at this stage. For example, *Bcl11a* but not *Bcl11b*, was expressed in the limb buds (Figure 4.2A1 and Figure 4.2B1). In contrast, *Bcl11b* but not *Bcl11a* was observed in the trigeminal ganglion and nascent palate shelf (Figure 4B2 and Figure 4.2B4).
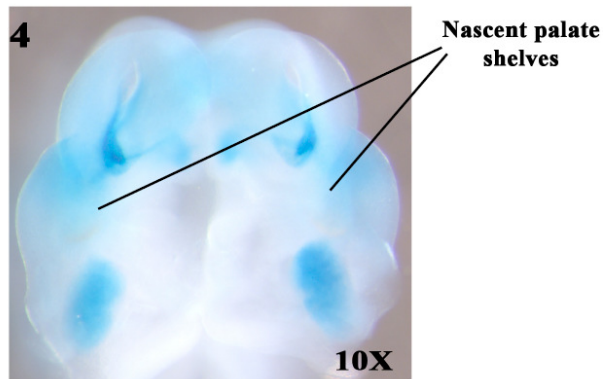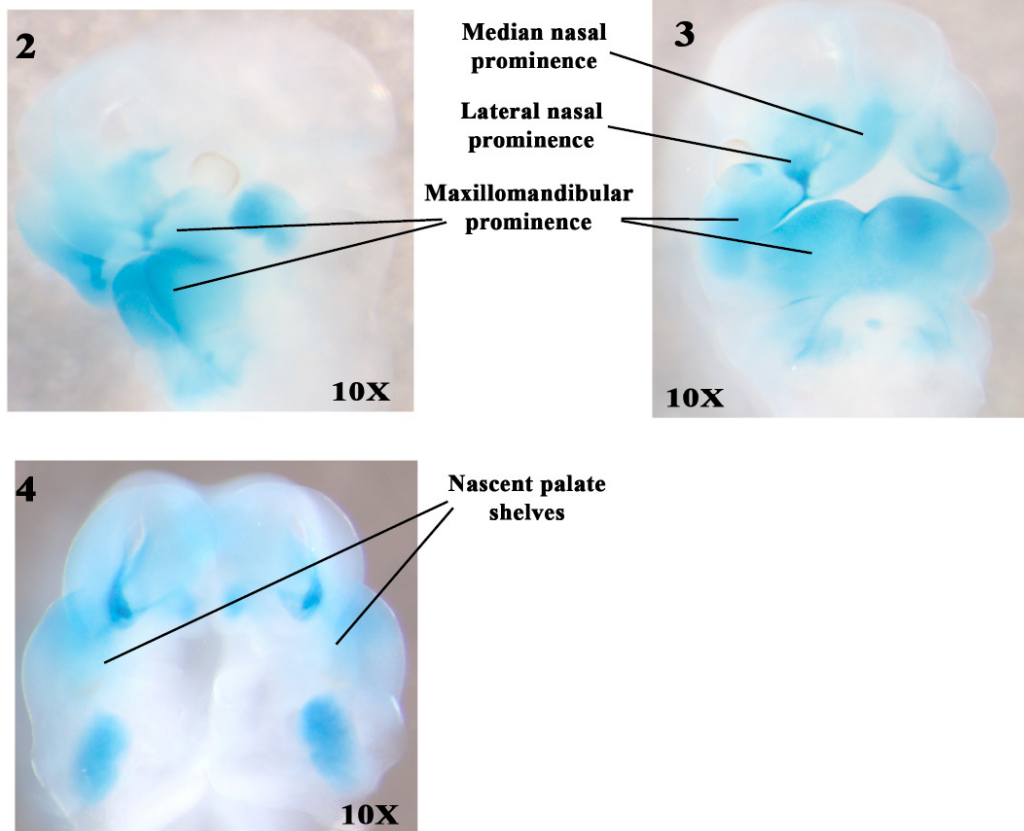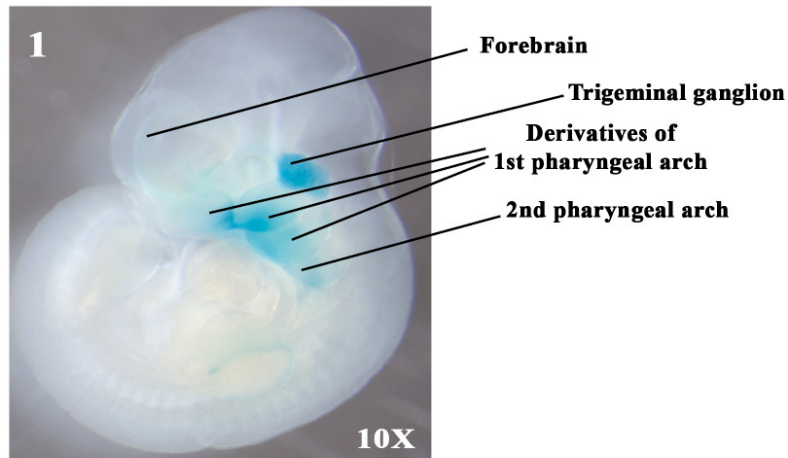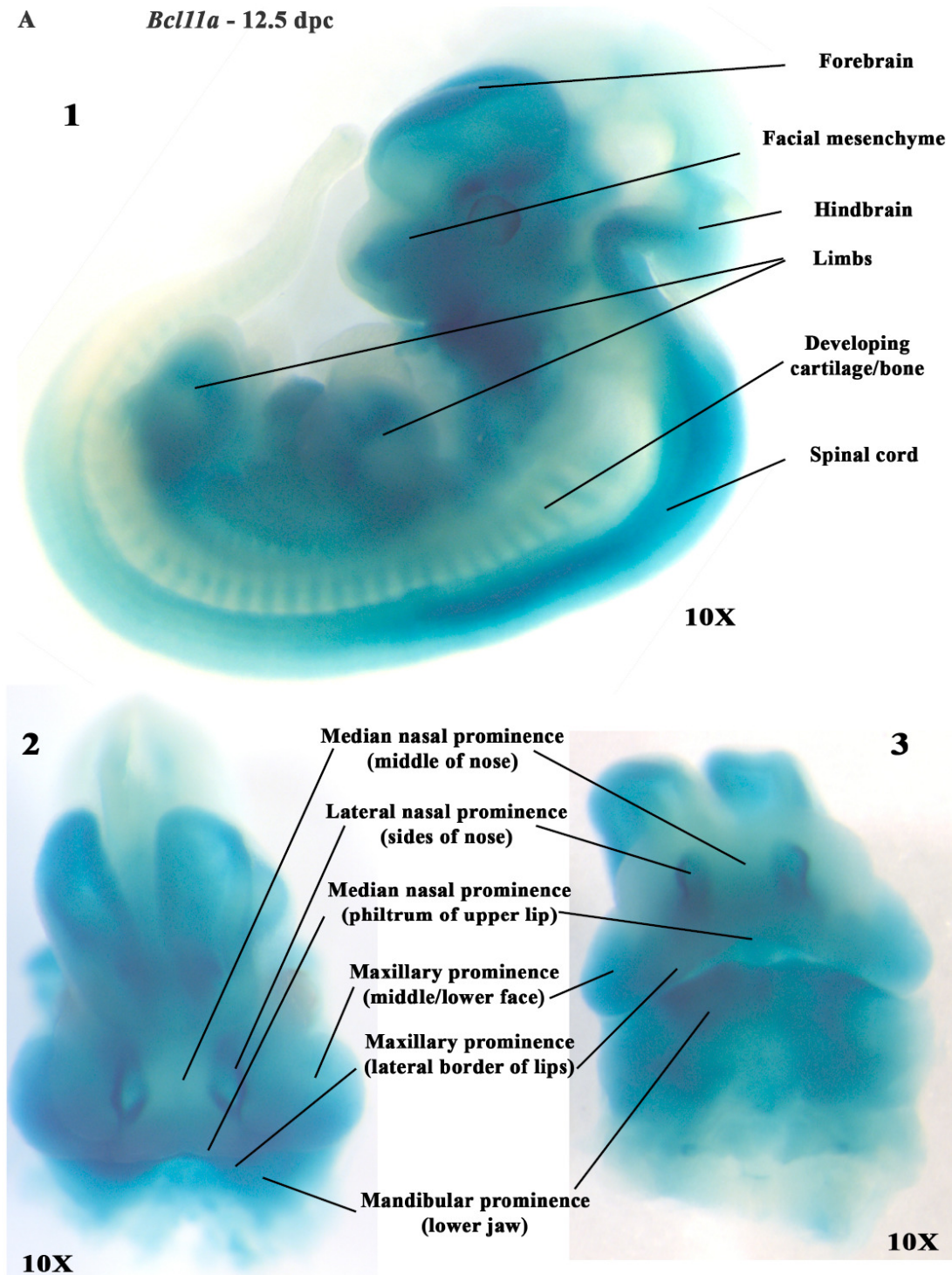
A

Bcl11a - 10.5 dpc

B   *Bcl11b* - 10.5 dpc

Figure 4.2. X-gal staining patterns of *Bcl11*^{lacZ/+} 10.5-11 dpc embryos. (A1) *Bcl11a* is expressed in pharyngeal arches, limb buds and forebrain from 10.5 dpc. **(A2-3)** Expression of *Bcl11a* is detected in the maxillomandibular, medial and lateral nasal prominence. **(B1)** *Bcl11b* is expressed in pharyngeal arches, forebrain and trigeminal ganglion from 10.5 dpc. **(B2-3)** In addition, expression of *Bcl11b* is also detected in the maxillomandibular, medial and lateral nasal prominence and in **(B4)** the nascent palate shelves.

4.2.3 *Bcl11* genes are highly expressed in the brain and craniofacial regions

The expression patterns of both *Bcl11a* and *Bcl11b* were maintained at 12.5 dpc (Figure 4.3). Highest levels of *Bcl11* expression were detected in the central nervous system and the craniofacial mesenchyme. Within the brain, expression of *Bcl11a* was detected in the developing fore- and hind-brain (Figure 4.3A1). *Bcl11a* was found to be highly expressed in the lateral and median nasal prominence, the maxillary prominence and the mandibular prominence within the facial mesenchyme (Figure 4.3A2 and 4.3A3). Expression of *Bcl11b* in the facial mesenchyme overlapped with that of *Bcl11a*, suggesting that these genes might have complementary role(s) in development of the facial mesenchyme. In the brain, expression of *Bcl11b* was detected in the developing fore-brain (Figure 4.3B1-3). Intriguing, a differential spatial expression pattern of these two genes had begun to emerge at this stage. Within the CNS, while *Bcl11a* was highly expressed in the spinal cord (Figure 4.3A1); *Bcl11b* was found to be highly expressed in trigeminal ganglion and the dorsal root ganglion (Figure 4.3B1). This indicates that *Bcl11* genes may play different roles in development of specific regions of the CNS. Expression of *Bcl11* genes became more restricted from 14.5 dpc and high levels of expression were maintained in the CNS and craniofacial regions (Figure 4.4). Within the CNS, overlapping *Bcl11a* and *Bcl11b* expression was observed in forebrain (cerebral cortex), midbrain, hindbrain, the nasal epithelium and spinal cord (Figure 4.4A and 4.4B). Overlapping expression of *Bcl11* genes in the brain was maintained at 18.5 dpc (Figure 4.5) and in the adult (Figure 4.6). At 18.5 dpc, expression of both genes was observed in the cerebral hemisphere and in the medulla (Figure 4.5A and 4.5B). In the adult brain, expression of both genes was detected in cerebral cortex, olfactory bulb and in the cerebellum (Figure 4.6A1-2 and 4.6B1-2). Purkinje cells, which are large GABAergic neurons, are located within the purkinje cell layer of the cerebellum. These neurons extend dendritic projections upwards into the molecular layer and axonal projections downward to deep cerebellar nuclei. Purkinje cells are considered to be the principal output of the cerebellum controlling several components of descending motor pathways (Kreitzer and Regehr, 2001). Both *Bcl11* genes were expressed in the Purkinje cell layers (Figure 4.6A3 and 4.6B3). In summary, the unique expression of *Bcl11* genes is

maintained in the brain and craniofacial regions throughout embryonic and postnatal development, suggesting that *Bcl11* genes may play important, yet complementary roles in the brain.
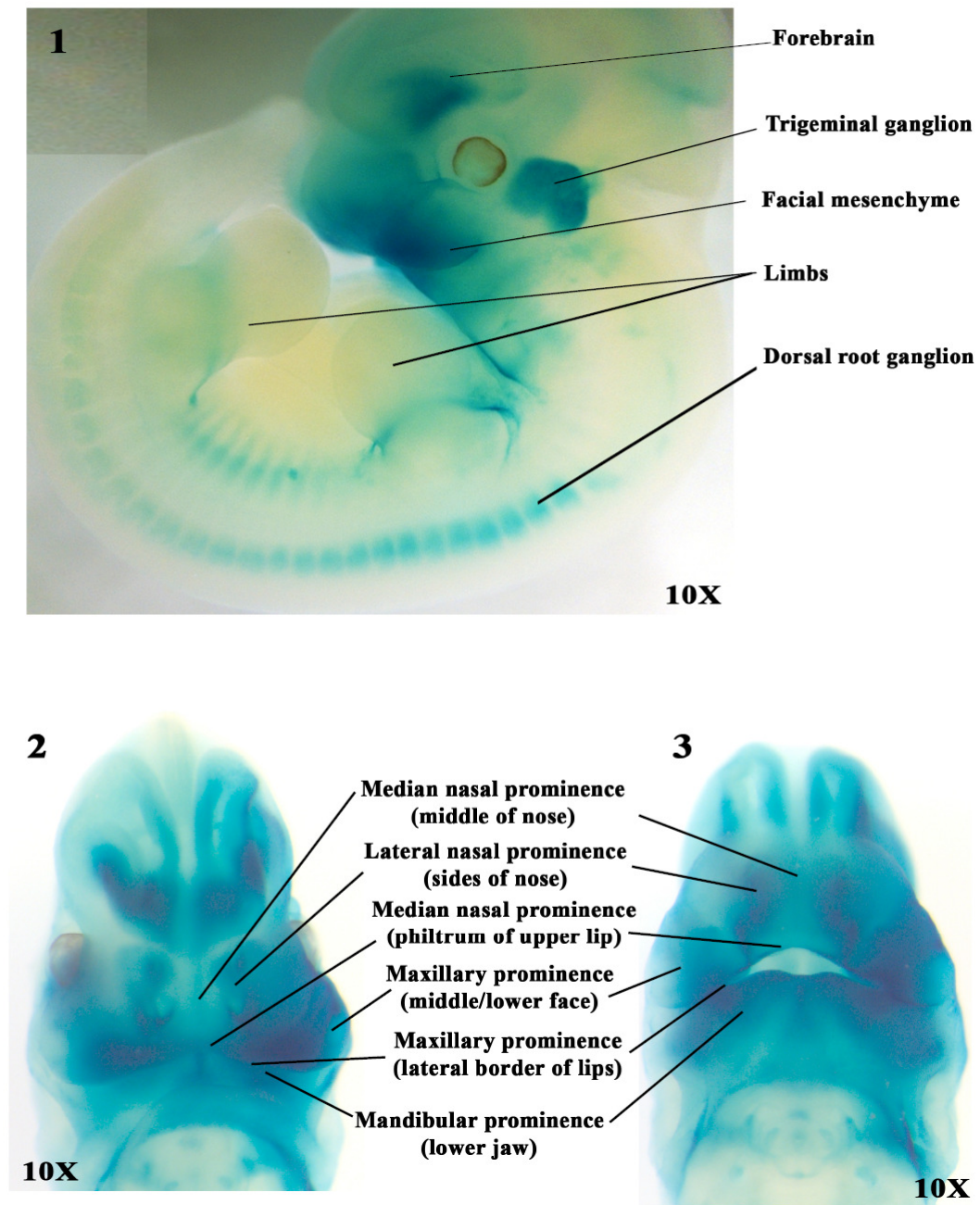

A   *Bcl11a* - 12.5 dpc

1

Forebrain

Facial mesenchyme

Hindbrain

Limbs

Developing cartilage/bone

Spinal cord

10X

2   3

Median nasal prominence
(middle of nose)

Lateral nasal prominence
(sides of nose)

Median nasal prominence
(philtrum of upper lip)

Maxillary prominence
(middle/lower face)

Maxillary prominence
(lateral border of lips)

Mandibular prominence
(lower jaw)

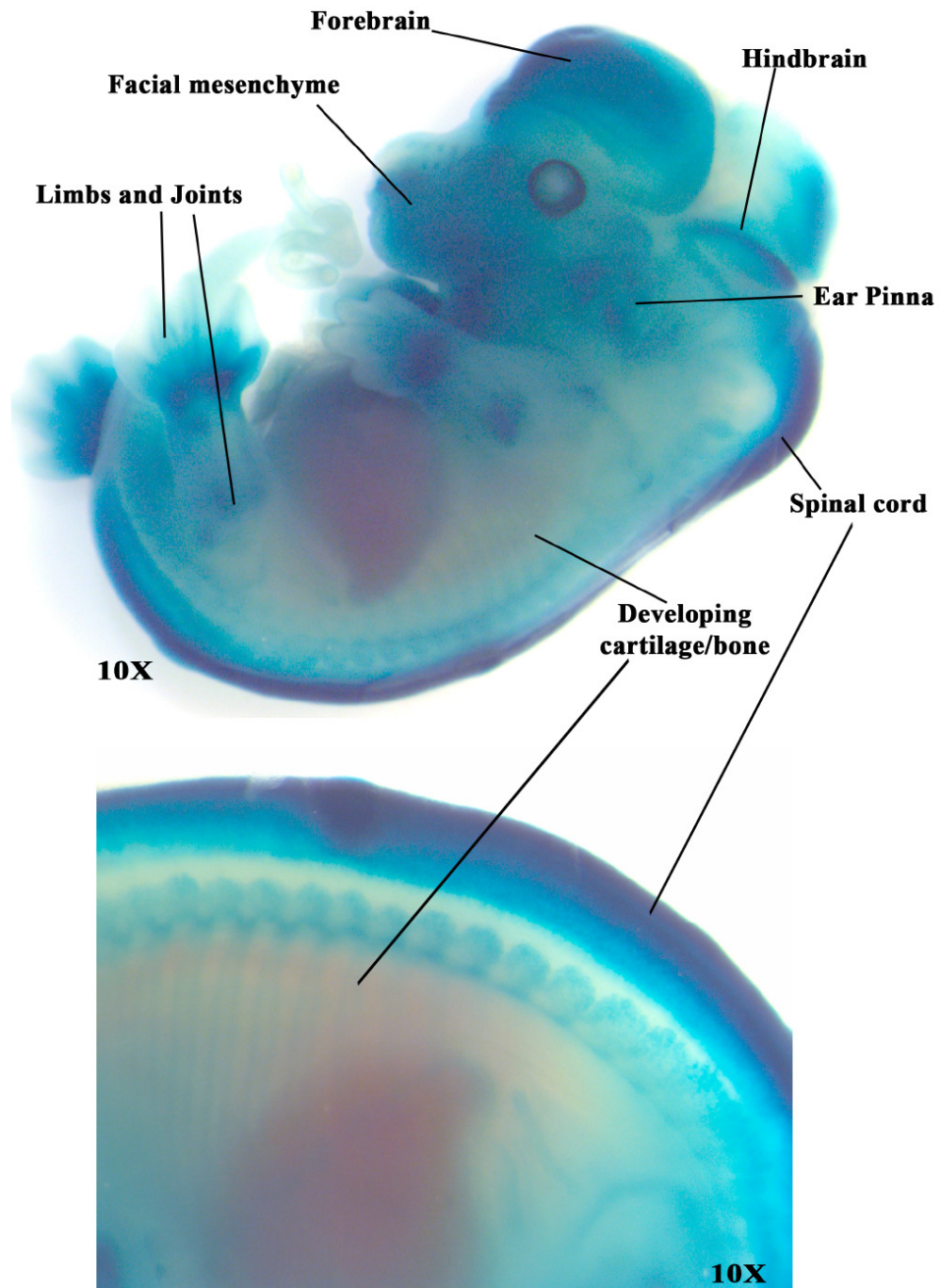10X   10X

B   *Bcl11b* - 12.5 dpc

Figure 4.3. X-gal staining patterns of *Bcl11*^*lacZ/+*^ 12.5-13 dpc embryos. (A1) *Bcl11a* is expressed in facial mesenchyme, limb buds, forebrain, hindbrain and spinal cord at 12.5 dpc. (A2-3) Expression of *Bcl11a* is maintained in all regions of the facial mesenchyme. (B1) *Bcl11b* is expressed in facial mesenchyme, forebrain, dorsal root ganglion and trigeminal ganglion from 12.5 dpc. (B2-3) In addition, expression of *Bcl11b* is also maintained in the facial mesenchyme, similar to *Bcl11a*.

145

A   *Bcl11a* - 14.5 dpc

Forebrain

Facial mesenchyme

Hindbrain

Limbs and Joints

Ear Pinna

Spinal cord

Developing
cartilage/bone
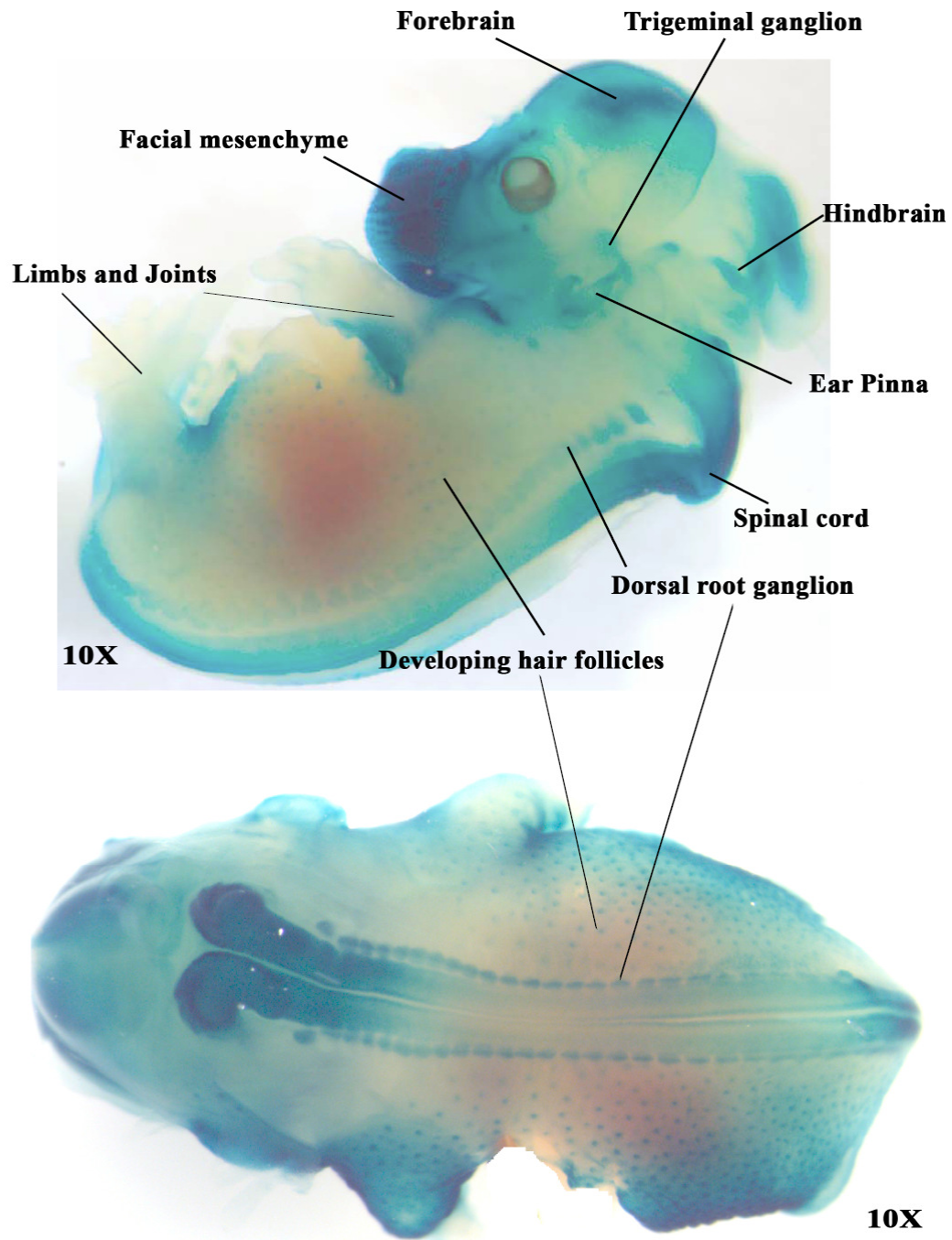
10X

10X

B   *Bcl11b* - 14.5 dpc

Figure 4.4. X-gal staining patterns of *Bcl11*$^{lacZ/+}$ 13.5-14.5 dpc embryos. (A) Expression of *Bcl11a* is maintained in facial mesenchyme, limbs and central nervous system. Expression of *Bcl11a* in facial mesenchyme is maintained. **(B)** Expression of *Bcl11b* is maintained in facial mesenchyme, central nervous system and also observed in hair follicles at 14.5 dpc.
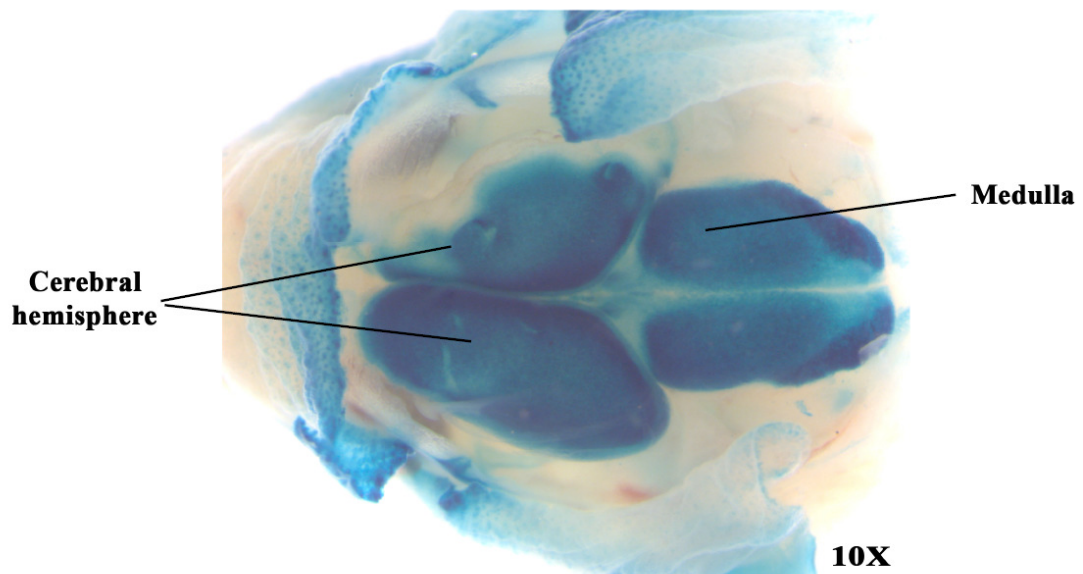
A   *Bcl11a* - 18.5 dpc

Medulla

Cerebral
hemisphere

10X

B   *Bcl11b* - 18.5 dpc

Medulla

Cerebral
hemisphere

10X
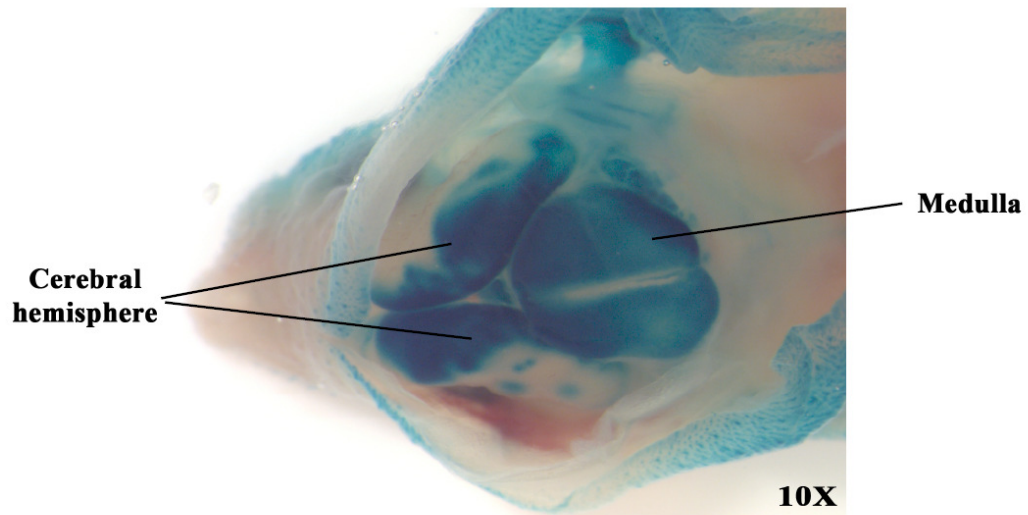
Figure 4.5. X-gal staining patterns of *Bcl11*$^{lacZ/+}$ 18.5 dpc embryos. (**A**) *Bcl11a* and (**B**) *Bcl11b* are highly expressed in cerebral hemispheres and medulla of the brain.

A *Bcl11a* - Adult

1

Olfactory bulb   Cerebral cortex   Cerebellum   **10X**

2

3

Purkinje cell layer   **10X**

B *Bcl11b* - Adult

1

Olfactory bulb   Cerebral cortex   Cerebellum   **10X**

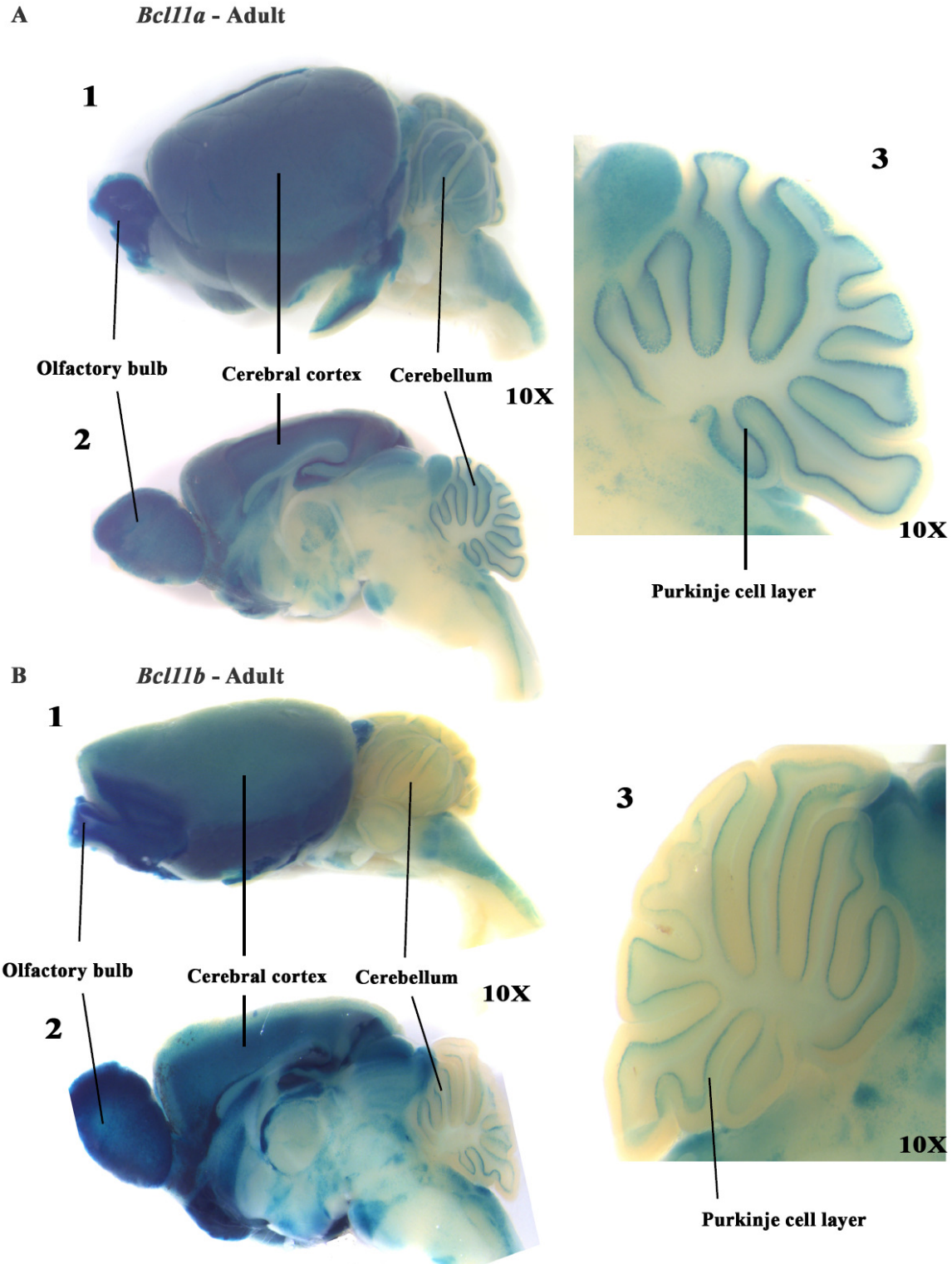**2**

3

10X

Purkinje cell layer

Figure 4.6. X-gal staining patterns of *Bcl11^{lacZ/+}* adult brain. Both (**A**) *Bcl11a* and (**B**) *Bcl11b* are highly expressed in the adult brain. Expression can be detected in the (**A1-2; B1-2**) olfactory bulb, cerebral cortex, cerebellum and also in (**A3 and B3**) purkinje cell layer of the cerebellum. **A1** and **B1** are lateral images of the brain while **A2** and **B2** are midline images of the brain. **A3** and **B3** are close-up images of the cerebellum.

4.2.4 *Bcl11* genes exhibit differential expression patterns in other tissues

Besides the craniofacial regions and the brain, expression of *Bcl11* genes was also detected in other tissues. At 12.5 dpc, *Bcl11a* but not *Bcl11b* was highly expressed in developing limb buds and cartilage/bone (Figure 4.3A1) which suggests that *Bcl11a* may play specific roles in limb and cartilage/bone formation. Similar to 12.5 dpc embryos, differential expression of *Bcl11* genes was maintained in the following regions: expression of *Bcl11a* was detected in the limbs and joints, developing cartilage/bones while expression of *Bcl11b* was detected in trigeminal ganglion at 14.5 dpc. Outside of the CNS, expression of both *Bcl11* genes was also detected in the ear pinna and the inner ear (Figure 4.4A and 4.4B), suggesting that *Bcl11* genes have roles in ear development. Additionally, *Bcl11b* was also found to be expressed in developing hair follicles (Figure 4.4B). This observation is consistent with the reported *Bcl11b* expression pattern using antibodies which showed that *Bcl11b* expression was detected in the rapidly dividing basal cell layer at 14.5 dpc (Golonzhka et al., 2007), suggesting that the possible involvement of *Bcl11b* in skin development.
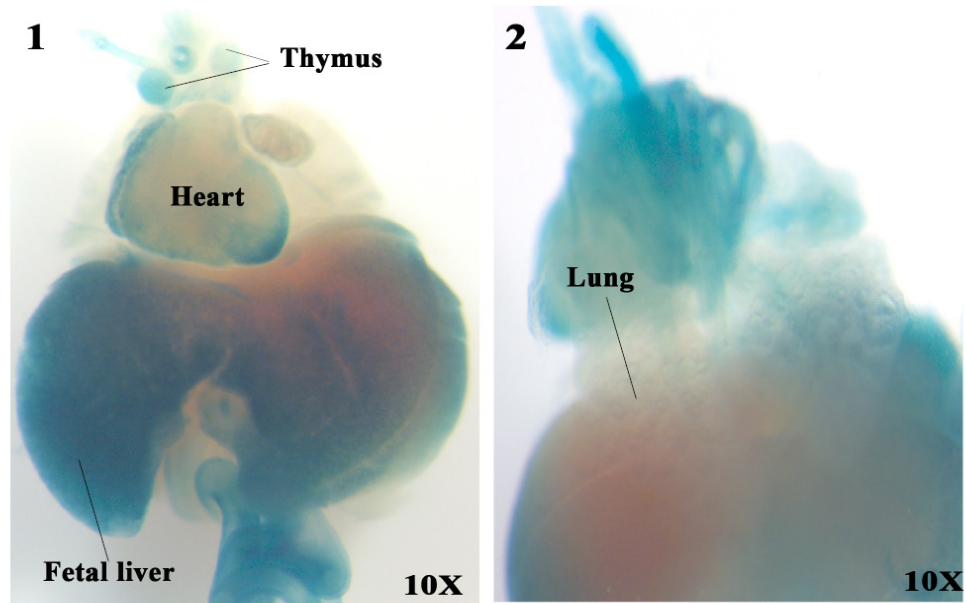
Analyses of X-gal staining patterns of internal organs of the $Bcl11a^{lacZ/+}$ 14.5 dpc embryos revealed that *Bcl11a* was expressed in the heart, fetal liver and weakly in the thymus but not in the developing lungs (Figure 4.7A1-2). Hematopoiesis begins in the aorta-gonad-mesonephros (AGM) region from 8.5 dpc and continues in the fetal liver where hematopoietic stem cells differentiate into myeloid and lymphoid lineages. Expression of *Bcl11a* in the fetal liver and in hematopoietic cells (See below, Chapter 4.2.7.2) is consistent with its essential roles in hematopoiesis. In contrast, analyses of $Bcl11b^{lacZ/+}$ 14.5 dpc embryos revealed that *Bcl11b* was expressed in the oesophagus and in the developing lung but not in the heart (Figure 4.7B1-2). Intrathymic T cell development begins when fetal liver derived progenitor cells seed the thymus where they expand and differentiate into mature T cells (Rothenberg, 2007a, b). Expression of *Bcl11b* was detected in the developing thymus at 14.5 dpc at a time when most thymocytes are CD4 and CD8 double negative (T cell precursors), and its expression was maintained at 18.5 dpc (Figure 4.8B1) and in the adult thymus (Figure 4.9B). In addition, expression of *Bcl11b* was detected in thymocytes from $CD44^{+}CD25^{-}$ DN1 stage during T

cell development (See below, Chapter 4.2.7.2). These expression data are consistent with the *Bcl11b* knockout phenotype where *Bcl11b* is essential for αβ T cell development (Wakabayashi et al., 2003b). In contrast, expression of *Bcl11a* was only detected at low levels in the thymus at 18.5 dpc (Figure 4.8A1) and the *Bcl11a$^{lacZ/+}$* adult thymus showed a punctate staining pattern (Figure 4.9A1). In the adult thymus, expression of *Bcl11a* was detected in only a small percentage of CD44$^+$CD25$^-$ thymocytes (DN1 stage) during T cell development (See below, Chapter 4.2.7.2). These observations, together with T cell defects in the *Bcl11a* knockout mice (Liu et al., 2003b) provide additional evidence that *Bcl11a* also plays an important role in T cell development.

Interestingly, dynamic reciprocal expression of *Bcl11* genes was detected in the developing lungs. Expression of *Bcl11a*, which was not detected in the lungs at 14.5 dpc, was detected at 18.5 dpc (Figure 4.7A2 and 4.8A2). In contrast, expression of *Bcl11b* was detected at 14.5 dpc and not in the lungs at 18.5 dpc (Figure 4.7B2 and 4.8B2). These dynamic expression patterns of *Bcl11* genes in the lungs highlight their potential roles during lung morphogenesis.

Taken together, *Bcl11a* and *Bcl11b* exhibit unique spatial and temporal expression patterns during embryonic development. Expression of both genes was detected from 10.5 dpc, with high levels of expression in the brain and derivatives of the first and second pharyngeal arches. The expression patterns in the brain and craniofacial mesenchyme were maintained right up to adulthood. Regions of differential *Bcl11* expression were observed in certain tissues, such as limbs, developing cartilage/bones, lungs, heart and thymus. Additionally, the differential expression patterns of *Bcl11* genes in the thymus were also maintained. *Bcl11a* was only expressed weakly in certain cells in the adult thymus while high levels of *Bcl11b* expression were maintained from the embryonic thymus to the adult thymus. Considered together, these findings suggest that these two genes may play complementary roles in the adult brain but not in the thymus.

A   *Bcl11a* - 14.5 dpc

1   Thymus

Heart

Fetal liver

10X

2

Lung

10X

B   *Bcl11b* - 14.5 dpc

1   Thymus

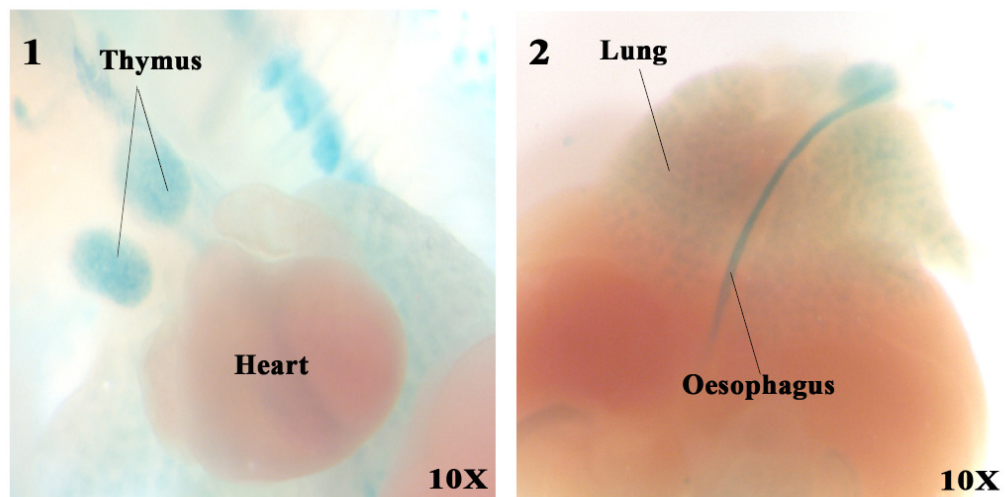Heart

10X

2   Lung

Oesophagus

10X

Figure 4.7. X-gal staining patterns of *Bcl11*$^{lacZ/+}$ 13.5-14.5 dpc tissues. Expression of *Bcl11a* is detected in the **(A1)** heart and thymus but not in the **(A2)** lungs. In contrast, expression of *Bcl11b* is not detected in the **(B1)** heart but only in the **(B1)** thymus and **(B2)** lungs.
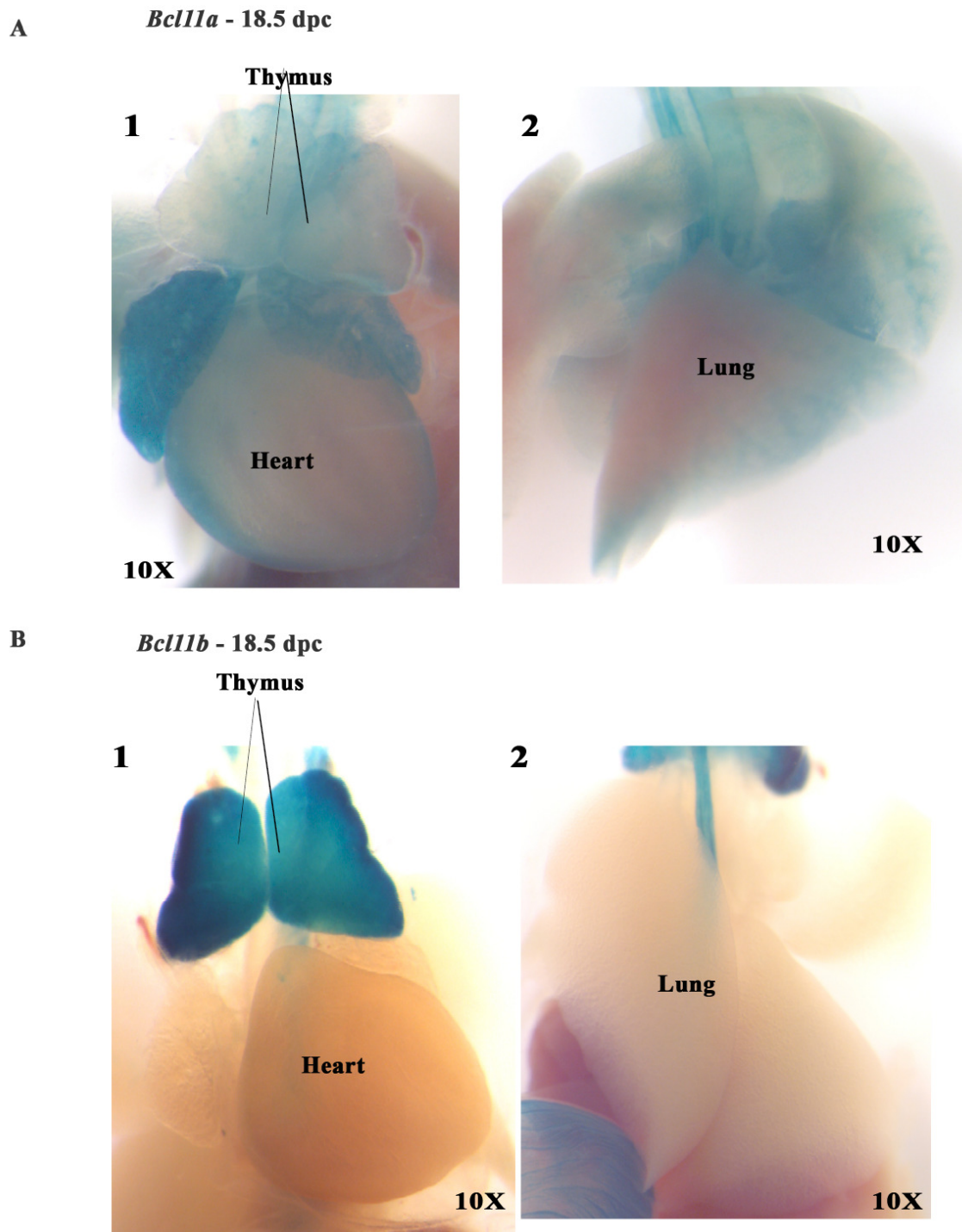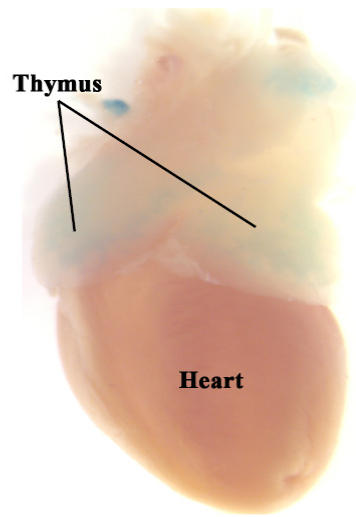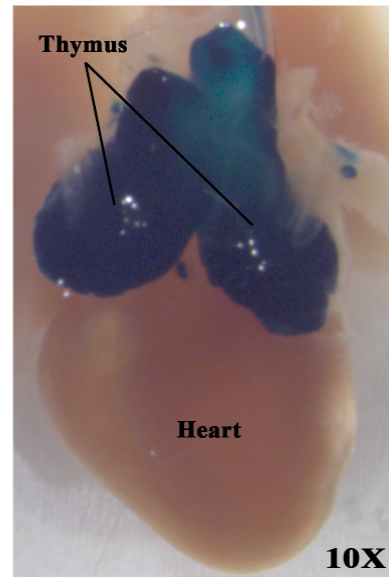
Figure 4.8. X-gal staining patterns of *Bcl11*^{lacZ/+} 18.5 dpc tissues. Expression of *Bcl11a* is maintained in the **(A1)** heart and certain regions of the thymus and also observed in **(A2)** certain regions of the lungs. Expression of *Bcl11b* is highly expressed in the **(B1)** thymus but not detected in the **(B1)** heart and **(B2)** lungs.

A   *Bcl11a* - Adult   **B**   *Bcl11b* - Adult

Figure 4.9. X-gal staining patterns of *Bcl11*^lacZ/+^ adult tissues. (A) Expression of *Bcl11a* is detected only in certain regions of the thymus but not in the heart. (B) *Bcl11b* is highly expressed in the thymus but not in the heart.

4.2.5 *Bcl11* genes are expressed specifically in embryonic mammary gland

Mammary gland development in the mouse is first observed at 10.5 dpc with the appearance of milk lines in both male and female embryos. The milk lines are two ridges of ectodermal thickenings that run in an anteroposterior (AP) direction between the fore- to the hind-limbs (Watson and Khaled, 2008). The development of the milk lines can be visualized using *in situ* hybridization with the *Wnt10b* and the *Lef1* probes (Foley et al., 2001; Veltmaat et al., 2004). These two genes are the earliest known markers of embryonic mammary development. Interestingly, expression of *Bcl11b* was detected in the presumptive regions of milk lines between the thoracic and inguinal regions at 10.5 dpc (Figure 4.10). Faint blue X-gal staining was observed to arise in an AP direction between the fore- and hind-limbs. No expression of *Bcl11a* was detected in the milk lines at 10.5 dpc. These observations indicated that *Bcl11b* is also one of the earliest genes to be specifically expressed in the milk lines at 10.5 dpc.

Mammary development becomes more distinctive from 11.5 dpc with the formation of five pairs of mammary placodes, each appearing in a specific order. By 12.5 dpc, the placodes have invaginated to form mammary buds (Watson and Khaled, 2008). Expression of *Bcl11a* remained undetectable in the mammary buds until 13.5-14.5 dpc (Figure 4.11A and 4.12A). Interestingly, expression of *Bcl11a* appeared to be in the surrounding mesenchyme of the mammary buds at 13.5-14.5 dpc (Figure 4.12A). After the initial expression in the milk line, *Bcl11b* became specifically expressed in developing mammary buds from 12.5 dpc (Figure 4.11B). This expression was maintained at 13.5-14.5 dpc where all five pairs of mammary buds expressed high levels of *Bcl11b* (Figure 4.12B). In summary, expression of *Bcl11b* started in the milk line at 10.5 dpc and from 12.5 dpc, its expression was detected in all the mammary buds. In contrast, expression of *Bcl11a* was detected only from 13.5 dpc onwards and its expression appeared to be in the mesenchyme of the mammary buds. These results clearly demonstrate that *Bcl11* genes are expressed in mammary lineages during early embryonic development.
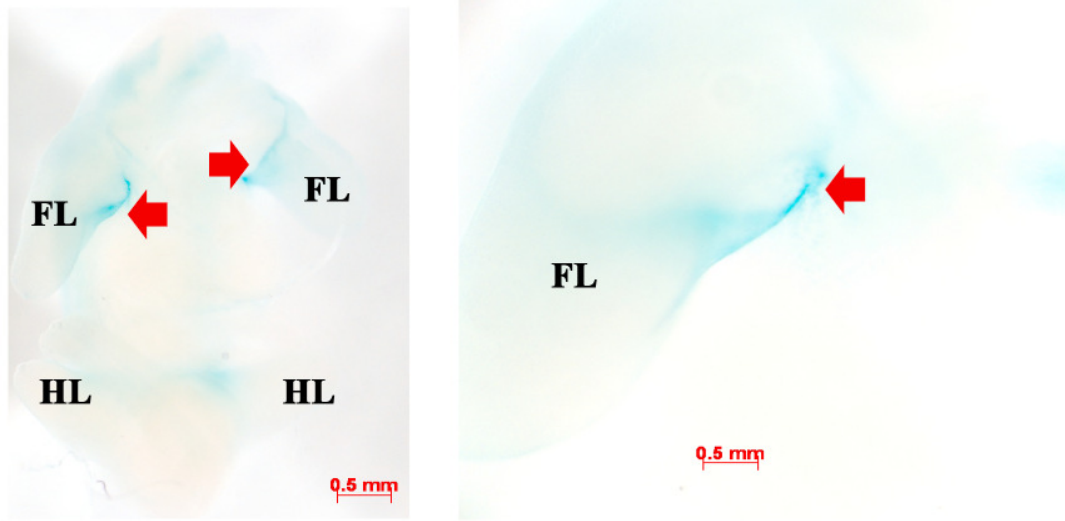
Bcl11b - 10.5 dpc

Figure 4.10. Expression of *Bcl11b* in milk line at 10.5 dpc. Expression of *Bcl11b* is detected in both the thoracic and inguinal milk lines from 10.5 dpc. Arrows indicate faint blue staining in the thoracic milk lines.

A   *Bcl11a* - 12.5 dpc
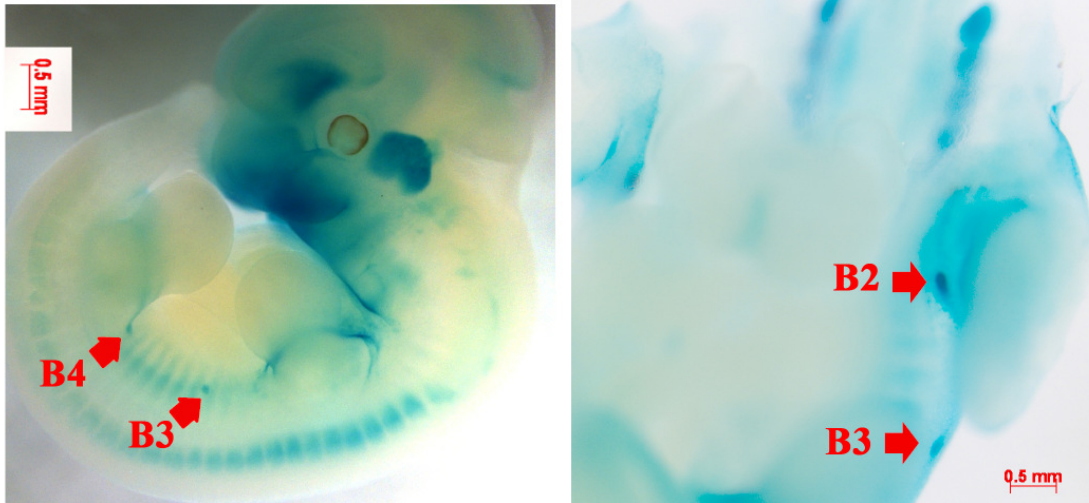

B   *Bcl11b* - 12.5 dpc
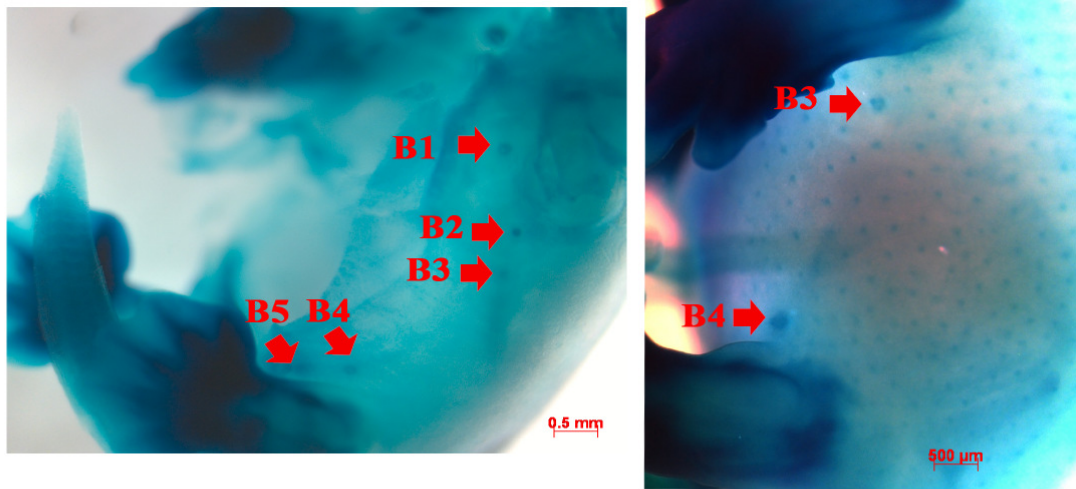

Figure 4.11. Expression of *Bcl11* genes in mammary lineages at 12.5 dpc. **(A)** Expression of *Bcl11a* is not detected at 12.5 dpc. **(B)** In contrast, expression of *Bcl11b* can be observed specifically in the mammary buds from 12.5 dpc. Arrows indicate positions of mammary buds. B2: 2nd pair of mammary buds; B3: 3rd pair of mammary buds; B4: 4th pair of mammary buds.

A   *Bcl11a* - 13.5 -14.5 dpc
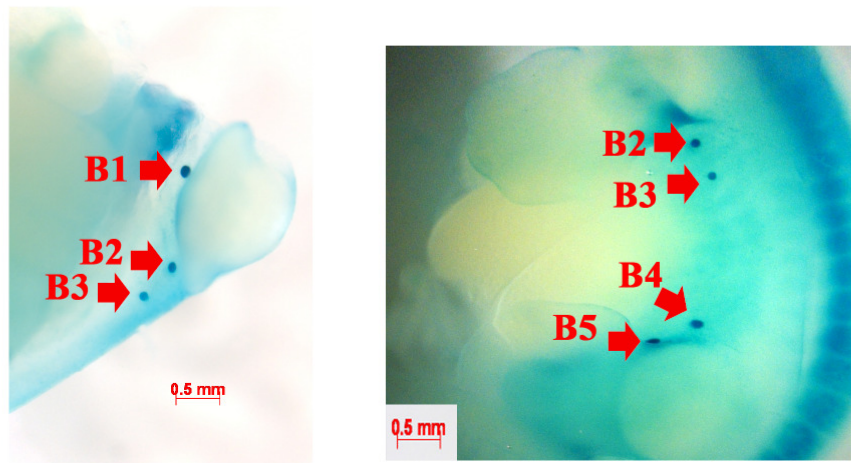

B   *Bcl11b* - 13.5-14.5 dpc

Figure 4.12. Expression of *Bcl11* genes in mammary lineages at 13.5-14.5 dpc. (A) Expression of *Bcl11a* is only detected in mammary buds from 13.5 dpc. Expression can be detected in all five pairs of mammary buds. Expression of *Bcl11a* appears to be predominantly in the surrounding mesenchyme.of mammary buds. **(B)** In contrast, expression of *Bcl11b* is detected in all five pairs of mammary buds. Arrows indicate positions of mammary buds. B1: 1st pair of mammary buds; B2: 2nd pair of mammary buds; B3: 3rd pair of mammary buds; B4: 4th pair of mammary buds; B5: 5th pair of mammary buds.

4.2.6 *Bcl11* genes exhibit unique and dynamic expression patterns in the mammary gland

4.2.6.1 *Bcl11a* is expressed in terminal end buds of mammary glands

Functional development of the mammary gland occurs in distinct stages; during embryonic development, the mammary anlage is established. By 16 dpc, the rudimentary mammary gland has become arborized and the ductules have begun to invade the underlying fat pad. After birth, ductal elongation occurs at a rate proportional to the overall growth rate of the animal. Following the onset of puberty at around 4 weeks, accelerated ductal elongation and branching morphogenesis occur, stimulated by estrogen hormone secretion. At this stage, terminal end buds (TEBs) which are large club-shaped structures appear at the end of growing ducts. The TEBs bifurcate to give rise to side branches and also lead the invasion of the fad pad by the growing ducts. As shown in Figure 4.13A1, *Bcl11a* was expressed in TEBs while expression of *Bcl11b* was detected in the neck region of TEBs (Figure 4.13A2). TEBs are specialized structures consisting of an outer layer of cap cells and the inner multi-layered body cells (Humphreys et al., 1996). The body cells give rise to mammary luminal epithelial cells and the cap cells are believed to contain mammary progenitor cells and precursors of myoepithelial cells. Sections of X-gal stained $Bcl11a^{lacZ/+}$ 4-5 weeks old mammary glands revealed that expression of *Bcl11a* was detected in both the cap and body cells of TEBs (Figure 4.13A3). In contrast, expression of *Bcl11b* was only detected in some cells found in the cap cell layer which are destined to become the basal/myoepithelial layer (Figure 4.13A4).

A highly regulated process of cell proliferation and apoptosis occurs within the highly proliferative TEBs (Humphreys et al., 1996). This ultimately generates the mature mammary epithelium which consists of two main cell types: the luminal cells which line the innermost layer of the lumen and forms the ducts and secretory alveoli, and the basal/myoepithelial cells that surrounds the luminal cells and provide contractile forces to facilitate transport of the milk to the nipple. In the mature mammary gland (8-12 weeks), *Bcl11a* was found to be expressed in both luminal and basal cells as well as in the alveolar buds during estrus cycle (Figure 4.13B1 and B3). Expression of *Bcl11b*, on the

other hand was detected primarily in the basal/myoepithelial layers in the mature epithelium (Figure 4.13B2 and B4). The differential expression patterns of *Bcl11* genes in the virgin mammary epithelium suggest that *Bcl11a* may be important in the establishment of the luminal and basal lineages while *Bcl11b* may be important for the basal lineage.
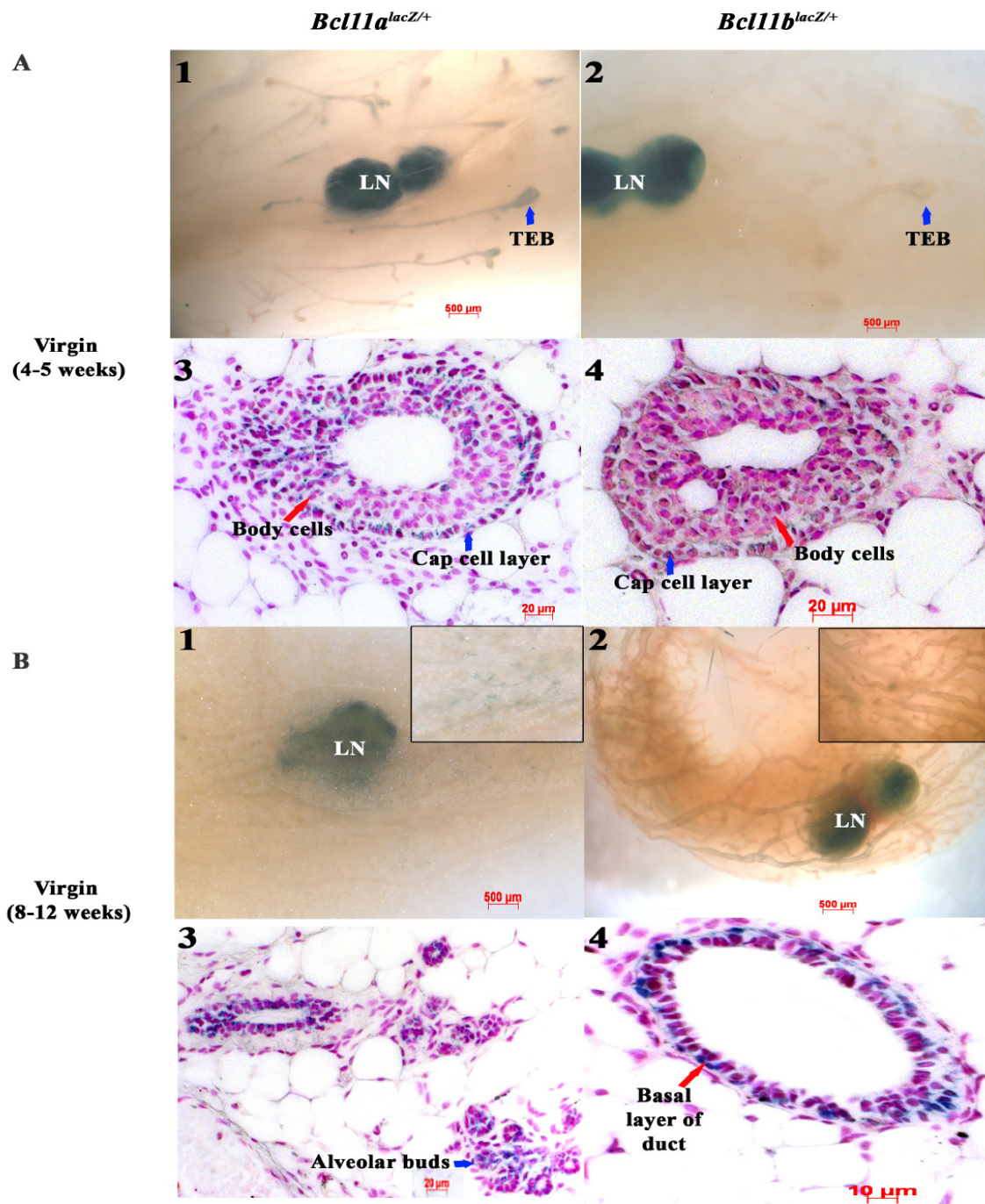
Figure 4.13. X-gal staining patterns of mammary tissues from *Bcl11*^lacZ/+^ virgin glands. (A1) *Bcl11a* is highly expressed in terminal end buds (TEBs) of 4-5 weeks old virgin mammary glands. **(A3)** Sections show that *Bcl11a* is expressed in both cap and body cells of TEBs. **(A2)** In contrast, *Bcl11b* is not expressed in TEBs but at the neck regions of TEBs. **(A4)** Sections show the expression of *Bcl11b* is restricted to few cap cells and the developing myoepithelial/basal layers. In mature virgin females (8-12 weeks), **(B1)** low levels of *Bcl11a* expression is detected in the differentiated alveolar structures observed during estrus cycles and **(B3)** sections indicate that *Bcl11a* is detected in both luminal and basal layers of the mammary glands. However, expression of *Bcl11b* is restricted predominantly to **(B2 and B4)** basal layers of the mammary glands. TEB indicates terminal end bud; LN indicates lymph node.

4.2.6.2 Differential expression of *Bcl11* genes during pregnancy, lactation and involution

During pregnancy, the mammary gland undergoes extensive proliferation, differentiation and remodelling in preparation for lactation in order to nurse the pups. An important morphological change in the mammary gland is the production of lobulo-alveolar structures which eventually form secretory epithelial cells that produce milk to feed the newborn pups. Progesterone and prolactin signalling are critical in preparing the gland for gestation and lactation. Progesterone induces extensive side-branching and alveologenesis, while prolactin promotes differentiation of the alveolar structures. The alveolar structures, which consist of alveolar luminal cells and the surrounding myoepithelial cells, might arise from bi-potent ductal progenitors, though there is evidence that a distinct alveolar progenitor population exists within the mammary lineage hierarchy (Smith and Boulanger, 2003). Early in gestation (day 4-5), extensive proliferation and side-branching occur within the mammary gland. At this stage, up-regulation of both *Bcl11* genes was observed in the mammary epithelium (Figure 4.14A). Expression of *Bcl11a* was observed in the ducts and in the differentiating lobulo-alveolar structures (Figure 4.14A1) while expression of *Bcl11b* was observed only in the mammary ducts and not in the lobulo-alveolar structures (Figure 4.14A2). Sections of X-gal stained *Bcl11$^{lacZ/+}$* gestation glands showed that *Bcl11a* was expressed in both the ductal luminal cells and in the differentiating alveoli (Figure 4.14A3) while expression of *Bcl11b* was restricted to the basal/myoepithelial layer of mammary ducts and not in alveolar cells (Figure 4.14A4). The differential expression patterns were maintained throughout gestation (Figure 4.14B1 and B2) where expression of *Bcl11a* was detected in luminal ductal and alveolar cells (Figure 4.14B3) while expression of *Bcl11b* remained restricted to the basal/myoepithelial layer of ducts (Figure 4.14B4). These results indicated that *Bcl11a* was highly expressed in differentiating luminal cells of the ducts and alveolar while expression of *Bcl11b* was found primarily in the basal/myoepithelial layer of mammary ducts, suggesting that *Bcl11a* may be important for luminal differentiation.

A lactogenic switch occurs during late pregnancy that is accompanied by the expression of milk proteins, whey acidic protein (WAP) and α-lactalbumin and by the

formation of lipid droplets (Watson and Khaled, 2008). During lactation, the mammary gland undergoes a morphological change. The alveolar structures become expanded that eventually filled up the entire mammary gland. The lumens of the alveoli become distended and filled with milk which is expelled from the secretory alveoli by the contraction of the myoepithelial layers surrounding the ducts and alveoli. Expression of *Bcl11a* was detected during lactation and sections of the X-gal stained *Bcl11a*$^{lacZ/+}$ day 3 lactation glands showed that *Bcl11a* was expressed in secretory luminal cells (Figure 4.15-1 and -3). Interestingly, not all the secretory luminal cells stained positive for *Bcl11a*. Expression of *Bcl11b* was undetectable during lactation (Figure 4.15-2 and -4).

Following lactation and weaning of the pups, the mammary gland undergoes a dramatic process involving apoptosis, dedifferentiation, tissue remodelling and immune infiltration called involution in order to remove the now redundant secretory cells (Watson, 2006a). At 72 hours post removal of the pups, expression of *Bcl11a* was present in the mammary gland undergoing involution (Figure 4.16-1). Surprisingly, *Bcl11b*, which was not detected during lactation, was up-regulated in the mammary gland at 72 hours post initiation of involution (Figure 4.16-2). Sections of X-gal stained *Bcl11*$^{lacZ/+}$ involution glands showed that *Bcl11* expression was detected in both epithelial cells and immune cells (Figure 4.16-3 and -4).

To confirm the X-gal staining, the expression changes of *Bcl11a* and *Bcl11b* during the adult mammary gland development cycle were determined using quantitative Real-Time PCR (qRT-PCR) (qRT-PCR performed by Dr Walid Khaled) (Figure 4.17). In total epithelial cells, there was dramatic up-regulation of *Bcl11* mRNA levels during early gestation. This is consistent with the X-gal staining patterns in the *Bcl11*$^{lacZ/+}$ adult mammary glands (Figure 4.14). *Bcl11a* mRNA levels remained high throughout gestation and lactation, suggesting that *Bcl11a* plays important roles in luminal epithelial cell differentiation. In contrast, *Bcl11b* expression levels decreased steadily over gestation and by lactation, its expression was virtually undetectable. During involution, there was a dramatic up-regulation of *Bcl11b* levels at 24 hours after initiation of involution, followed by a sharp decline before peaking again at 96 hours involution time point. These results suggest that *Bcl11b* plays important roles during involution, especially during the first phase of involution. On the other hand, levels of *Bcl11a* increased gradually during

involution and peaked at 72 hours involution, indicating that *Bcl11a* may also have a functional role during the second phase of involution. Taken together, qRT-PCR confirmed the dynamic expression of *Bcl11a* and *Bcl11b* during mammary gland development. These expression results laid the groundwork for the functional analysis of the roles of *Bcl11* genes in epithelial cell proliferation, differentiation and remodelling.
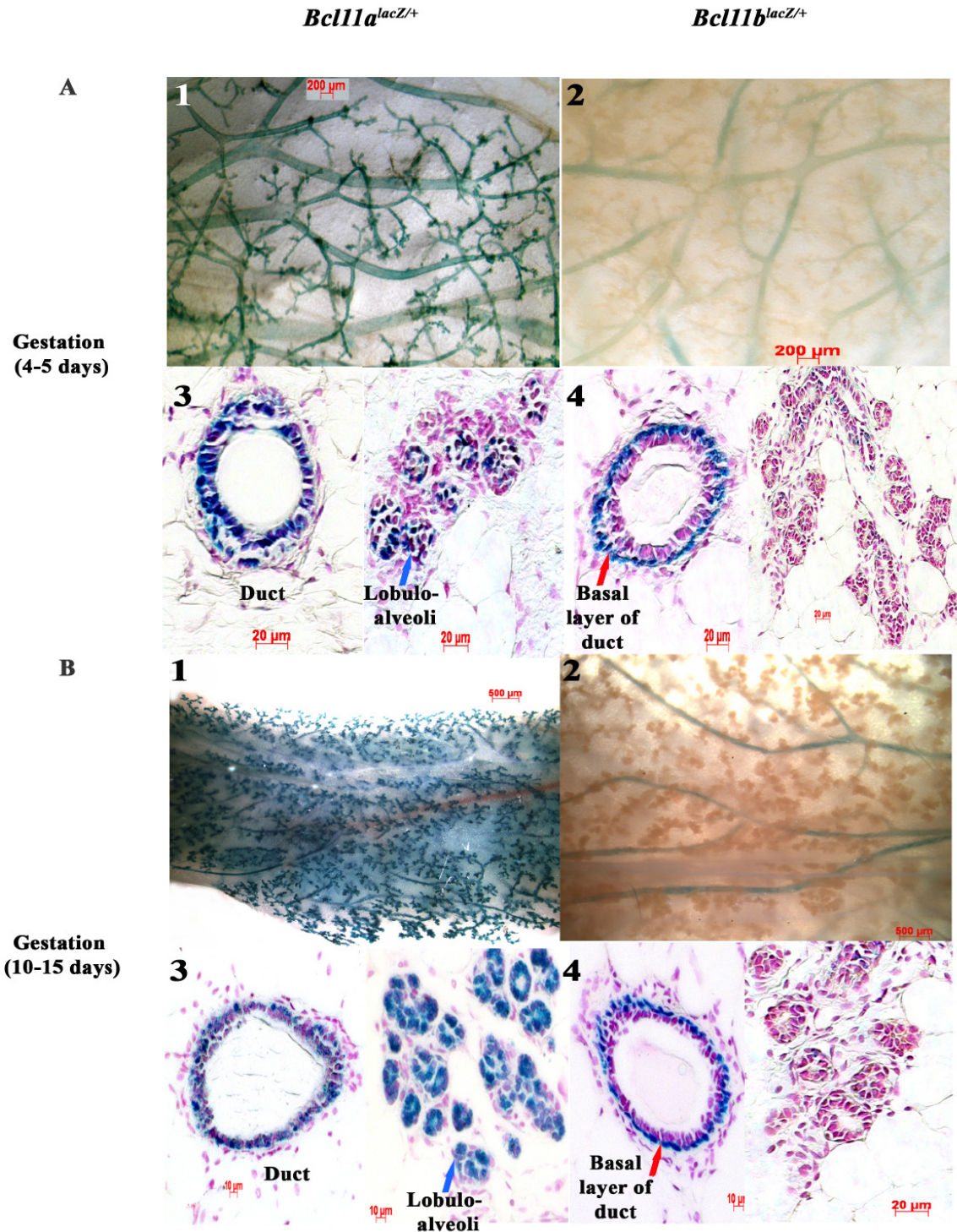
Figure 4.14. X-gal staining patterns of mammary tissues from $Bcl11^{lacZ/+}$ gestation glands. (A1-2) Both *Bcl11* genes are up-regulated during early gestation. **(A3)** Expression of *Bcl11a* is detected in both ductal luminal cells and in differentiating lobulo-alveolar structures. **(A4)** In contrast, expression of *Bcl11b* is detected only in ducts of the gestation glands and sections show that its expression is restricted primarily to basal layers of the ducts. **(B1-2)** The differential expression patterns are maintained throughout gestation. During late gestation, **(B3)** *Bcl11a* is detected in ductal cells and in differentiated lobulo-alveolar cells while **(B4)** *Bcl11b* is only detected in the basal layer of ducts but not in differentiated lobulo-alveolar cells.
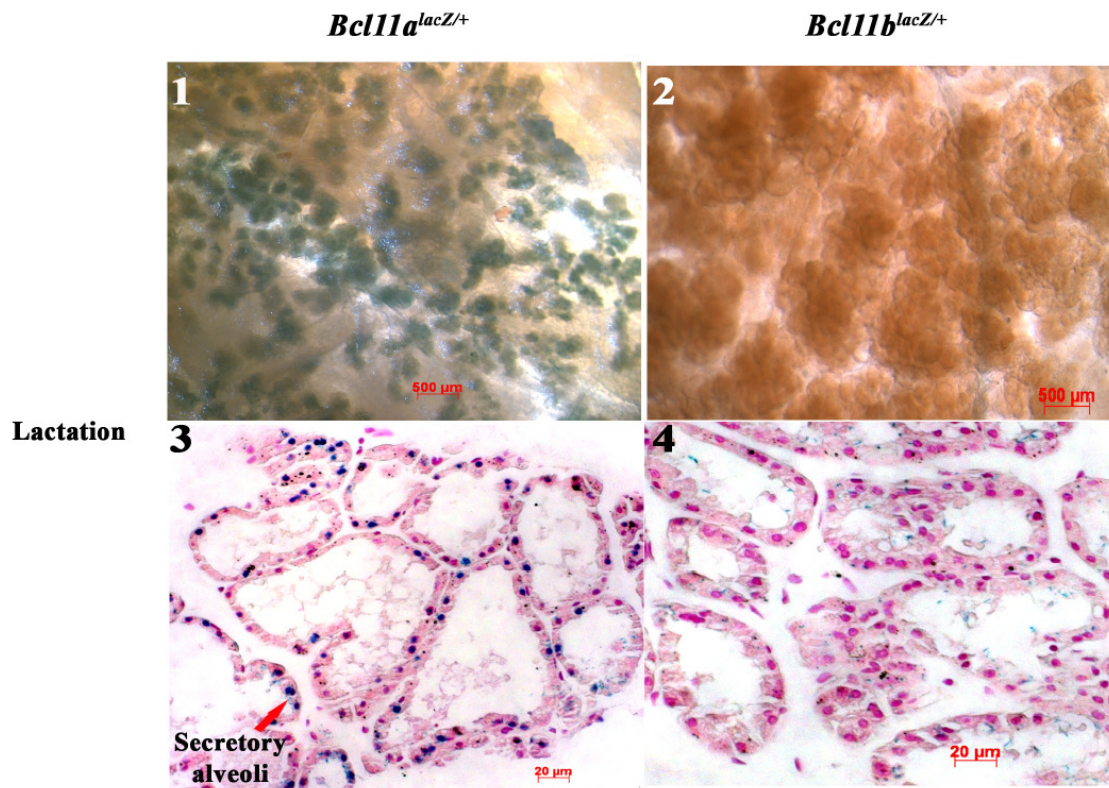
165

Figure 4.15. X-gal staining patterns of mammary tissues from *Bcl11^lacZ/+* lactation glands. (1-2) Only expression of *Bcl11a* is detected during lactation. *Bcl11a* expression is detected in lobulo-alveolar structures and sections show that **(3)** *Bcl11a* is expressed in secretory luminal cells. **(4)** Expression of *Bcl11b* is undetectable in secretory luminal cells.
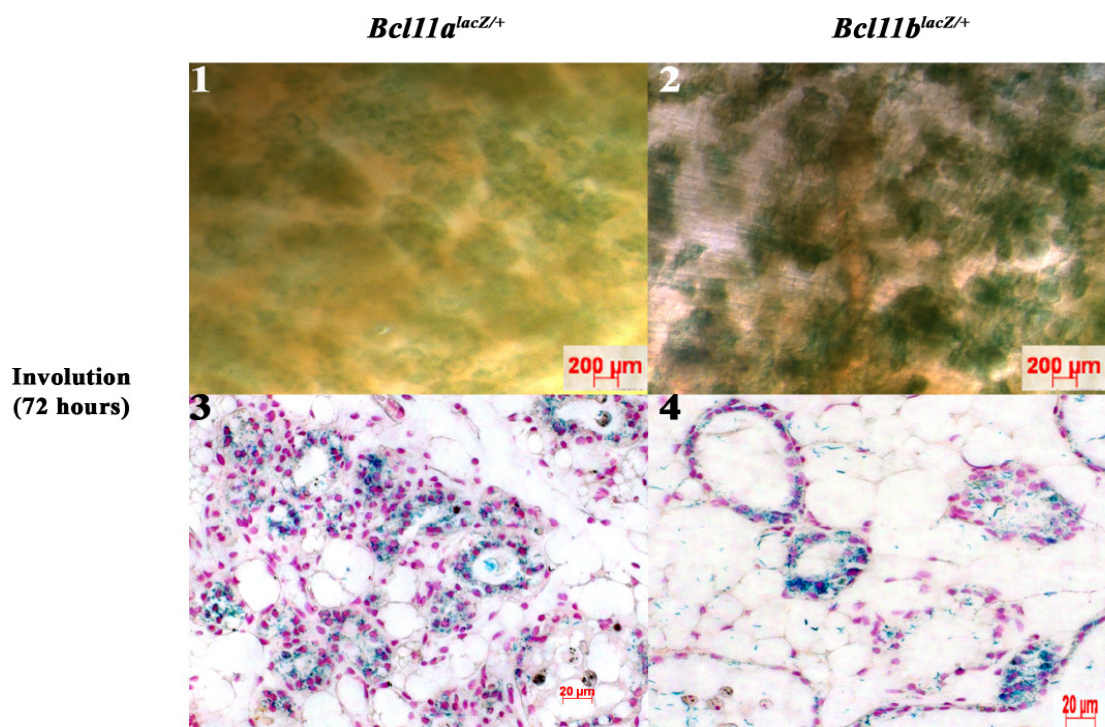
166

Figure 4.16. X-gal staining patterns of mammary tissues from *Bcl11*$^{lacZ/+}$ involution glands. (1-2) Expression of both *Bcl11* genes is detected during involution (72 hours). **(3-4)** Sections show that both genes are detected in some epithelial cells and also in the infiltrating immune cells.
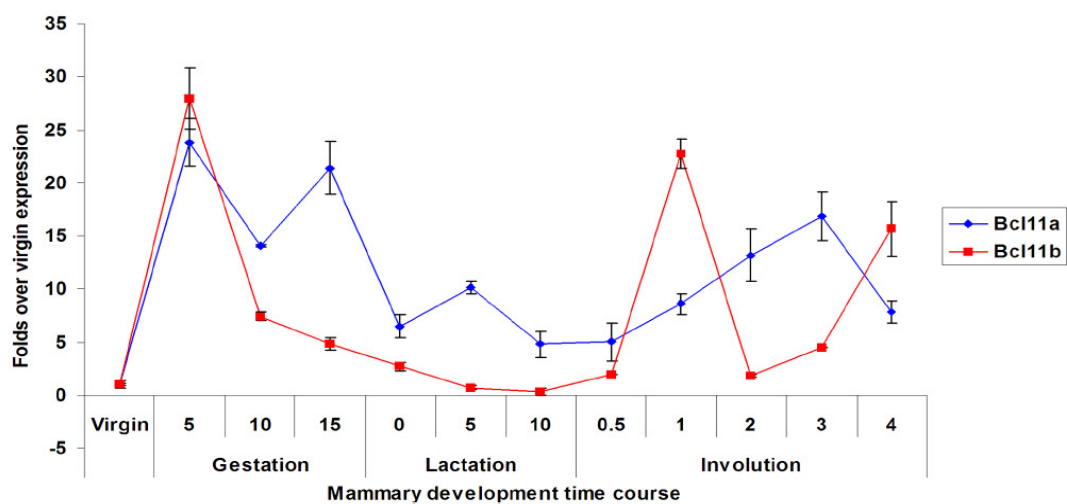

Figure 4.17. Expression patterns of *Bcl11* genes over Mammary Gland Development time course. Dynamic expression of *Bcl11* genes over mammary gland development time course as detected by quantitative real time PCR (qRT-PCR). Error bars denote standard deviation obtained from 3 independent samples. qRT-PCR performed by Dr Walid Khaled.

4.2.7   Expression of *Bcl11* genes in specific cell types
4.2.7.1 Characterization of *Bcl11$^{lacZ/+}$* mammary epithelial cells

The mammary gland is a ductal epithelial organ that consists of two epithelial cell types: luminal epithelial cells, which line the ductal lumen and secrete milk proteins, and the myoepithelial or basal cells, which line the basal surface of the luminal cells and interact with the stroma. Both types of cells are thought to arise from a multi-potent stem or progenitor population that has been recently characterized (Kordon and Smith, 1998; Shackleton et al., 2006; Stingl et al., 2006). The dichotomy in mammary epithelium bears many similarities to hematopoiesis whereby both B cells and T cells are believed to derive from the common lymphoid progenitors (CLPs). Indeed several studies have already demonstrated that genes involved in lymphoid lineage specification play important roles in the mammary gland (Asselin-Labat et al., 2007; Khaled et al., 2007; Kouros-Mehr et al., 2006). Similar to the field of hematopoiesis, the use of specific cell surface markers to delineate different populations of mammary epithelial cells has greatly facilitated characterization of the hierarchy of mammary epithelial population. Using antibodies to the heat stable antigen (CD24) in combination with either α6-integrin (CD49f) or β1-integrin (CD29), the mammary epithelial cells can be separated into the luminal (CD24^{hi}CD29f$^+$/CD49f$^+$) and basal/myoepithelial (CD24$^+$CD29f^{hi}/CD49f^{hi}) fractions using flow cytometry (Shackleton et al., 2006; Stingl et al., 2006) (Figure 4.18A).

To determine the expression of *Bcl11* genes in specific luminal and basal cell types, RT-PCR and qRT-PCR were performed on FACS-sorted mammary luminal/basal epithelial cells based on cell surface markers CD24 and CD49f (Stingl et al., 2006). The purity of each epithelial population was verified with lineage specific genes, *CK14* (basal) and *Muc1* (luminal). Consistent with the X-gal staining patterns as described above, *Bcl11a* transcripts were amplified from both the luminal and basal compartments of the virgin and gestation glands (Figure 4.18B). Up-regulation of *Bcl11a* expression was detected at day 5 gestation and this increase was predominantly in the luminal compartment (Figure 4.18B). Quantification using qRT-PCR showed that there was an approximately 10 fold increase in *Bcl11a* levels in the luminal compartment of the day 5 gestation gland compared to the virgin gland (Figure 4.18C). *Bcl11b* on the other hand

was amplified almost exclusively from the basal compartment in both the virgin and gestation glands (Figure 4.18B). Interestingly, there was a slight increase in the levels of *Bcl11b* in the luminal population during day 5 gestation as quantified by qRT-PCR (Figure 4.18C). As shown in Figure 4.19C, expression of *Bcl11b* in luminal lineages was detected in a small number of Sca1$^-$ (ERα$^-$) putative alveolar progenitors. Therefore the increase of *Bcl11b* in the luminal fraction was most likely attributed to the expansion of putative alveolar progenitor population during early gestation.

To further reveal the expression of *Bcl11a* and *Bcl11b* in the mammary epithelium, I stained the epithelial cells with antibodies to several cell surface markers and incubated them with FDG before analysis with flow cytometry. FDG is a fluorescent substrate of β-galactosidase for detecting its activity in live cells and can be used to determine the expression of *Bcl11* genes in specific mammary epithelial cells. Consistent with the whole mount X-gal staining and RT-PCR, *Bcl11a$^{lacZ/+}$* FDG positive epithelial cells in mice were located within both luminal (CD24^{hi}CD49f$^+$) and basal (CD24$^+$CD49f^{hi}) compartments while the *Bcl11b$^{lacZ/+}$* FDG positive epithelial cells were distributed primarily in the basal compartment where the mammary stem cells (MaSC) and progenitor cells are thought to be localized (Stingl et al., 2006) (Figure 4.19A). Expression of *Bcl11a* was detected in about 14.3 $\pm$ 1.8 % of luminal cells and 6.8 $\pm$ 0.9% of basal cells. In contrast, expression of *Bcl11b* was detected in only 2.1 $\pm$ 1.2% of luminal cells and 6.8 $\pm$ 0.3% of basal cells.

I then analyzed the *Bcl11$^{lacZ/+}$* FDG positive luminal epithelial cells (CD24^{hi}) in greater detail based on cell surface markers CD49b (α2-integrin) and Sca1 (Ly-6A/E) (Figure 4.19B). Luminal mammary epithelial cells can be classified into progenitor (CD49b$^+$) or differentiated (CD49b$^-$) cells based on the presence or absence of CD49b (Stingl and Watson; manuscript in preparation). The luminal progenitor population can be separated into Sca1$^-$ and Sca1$^+$ luminal progenitors. The CD49b$^+$Sca1$^+$ luminal progenitor subset has high levels of ERα expression while almost all the CD49b$^+$Sca1$^-$ cells are ERα-negative (Stingl and Watson; manuscript in preparation). Further analysis of the Sca1$^-$ and Sca1$^+$ luminal progenitors revealed that the Sca1$^-$ fraction has high levels of expression of milk proteins. These results conclude that there are two functionally distinct luminal progenitor populations in the mammary epithelium and it has been

postulated that the CD49b$^+$Sca1$^-$ (ERα-negative) subset represents putative alveolar progenitors while the CD49b$^+$Sca1$^+$ (ERα-positive) subset represents putative ductal progenitors (Stingl and Watson; manuscript in preparation).

Flow cytometric analysis revealed that that *Bcl11a$^{lacZ/+}$* FDG positive luminal epithelial cells (Lin$^-$CD24^{hi}FDG$^+$) were distributed in both progenitor (CD49b$^+$) and differentiated (CD49b$^-$) regions of the FACS profile (Figure 4.19C), indicating that *Bcl11a* was expressed in both luminal progenitors and differentiated luminal epithelial cells. In contrast, there were very few *Bcl11b$^{lacZ/+}$* FDG positive luminal epithelial cells (Lin$^-$CD24^{hi}FDG$^+$, 2.1% of luminal epithelial cells) and these Lin$^-$CD24^{hi}FDG$^+$ cells were distributed almost exclusively within the luminal progenitor (CD49b$^+$) regions of the FACS profile (Figure 4.19C). Expression of *Bcl11a* was detected in about 23.3 $\pm$ 6.3% of the total Sca1$^-$ (ERα$^-$) luminal progenitors while expression of *Bcl11b* was detected in only 2.9 $\pm$ 0.4% of the same population. In the luminal progenitor population, expression of *Bcl11a* was detected in 14.1 $\pm$ 2.9% of total Sca1$^+$ (ERα$^+$) luminal progenitors while expression of *Bcl11b* was detected in 2.3 $\pm$ 2.3% of the same population. Taken together, these results show that *Bcl11a* is expressed in luminal progenitors (both Sca1$^+$ and Sca1$^-$ progenitors) and in differentiated luminal cells. On the other hand, the few *Bcl11b* positive luminal cells are found within the Sca1$^-$ putative alveolar progenitor population.

Mammary glands contain different types of progenitor cells that can be detected under various conditions *in vitro* (Dontu et al., 2003; Smalley et al., 1998; Stingl et al., 2001). Mammary colony forming cells (Ma-CFCs) refer to progenitors that can form discrete mammary colonies *in vitro* (Stingl et al., 2001). In the mouse mammary epithelium, most Ma-CFCs are localized within the CD24^{hi}CD49f^{lo} subpopulation of luminal cells (Stingl et al., 2006). Accordingly, I sorted out mammary epithelial cells based on *Bcl11a* and *Bcl11b* expression, and assayed for their Ma-CFC capabilities. I found that *Bcl11a*-expressing epithelial cells had a 6-fold enrichment in Ma-CFC cloning efficiencies over non-*Bcl11a*-expressing cells (p<0.0011), further confirming that many luminal progenitors express *Bcl11a* (Figure 4.19D). No enrichment in Ma-CFC cloning efficiencies was observed for *Bcl11b*-expressing luminal cells (Figure 4.19D).
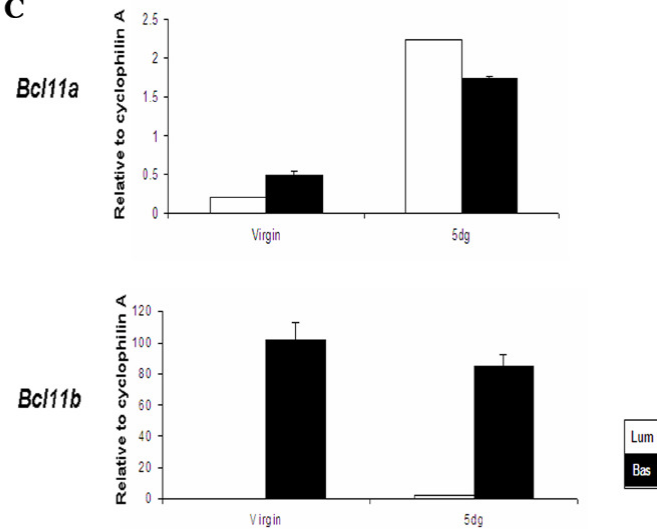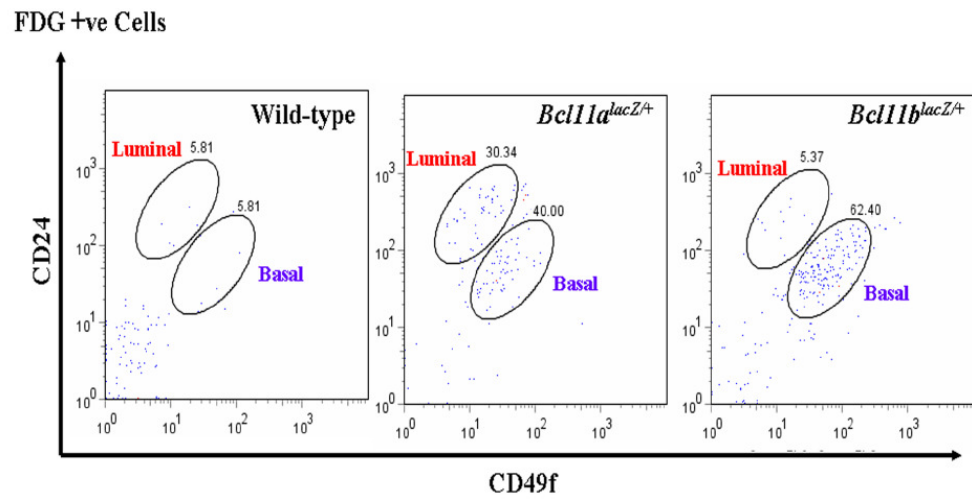
A
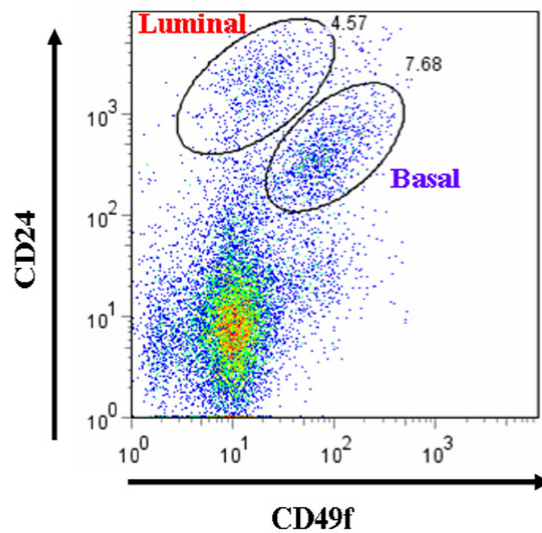
B
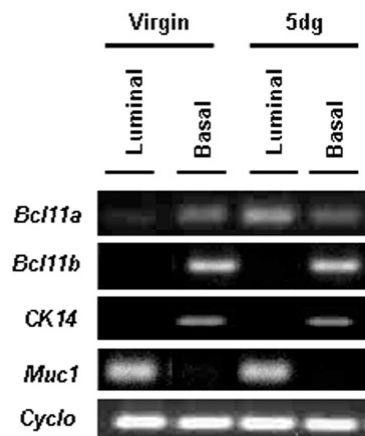
C

Figure 4.18. Expression of *Bcl11* genes in mammary epithelial cells. (**A**) Typical CD24 and CD49f mammary FACS profile of wild-type lineage-negative mammary epithelial cells. (**B**) Expression of *Bcl11* transcripts in sorted CD24^{hi}CD49f$^+$ (luminal) and CD24$^+$CD49f^{hi} (basal) fractions from virgin and day 5 gestation (5dg) mammary gland. Purity of sorted cells determined by *Muc1* (luminal) and *CK14* (basal) markers. (**C**) qRT-PCR confirmation of *Bcl11* expression in sorted CD24^{hi}CD49f$^+$ (luminal) and CD24$^+$CD49f^{hi} (basal) fractions from virgin and day 5 gestation mammary gland.

A

FDG +ve Cells

B

Sca1+ luminal progenitors (ERα+)
Sca1– luminal progenitors (ERα-)
Differentiated luminal cells

C

CD24^{hi} FDG +ve Cells

Sca1+ luminal progenitors (ERα+)
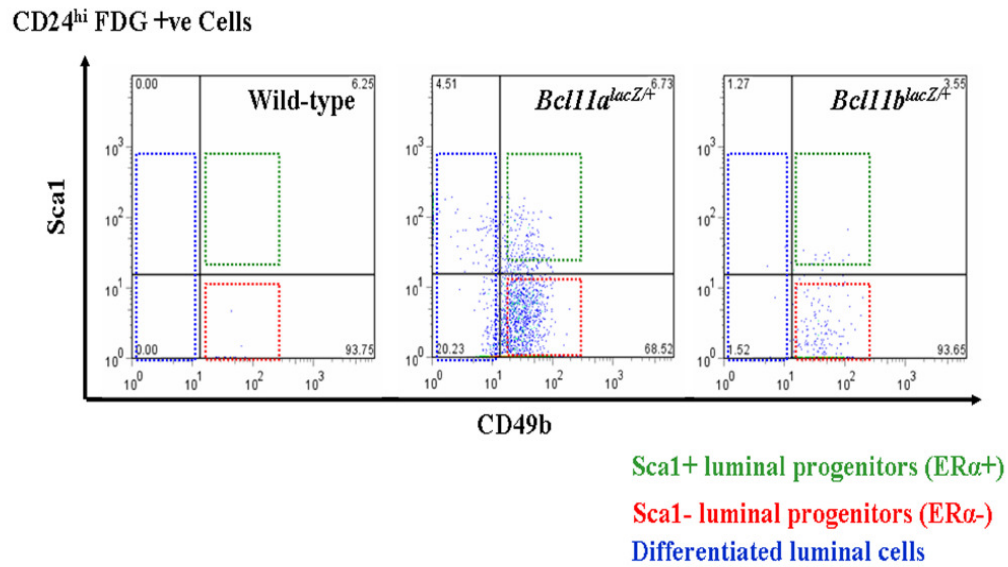Sca1- luminal progenitors (ERα-)
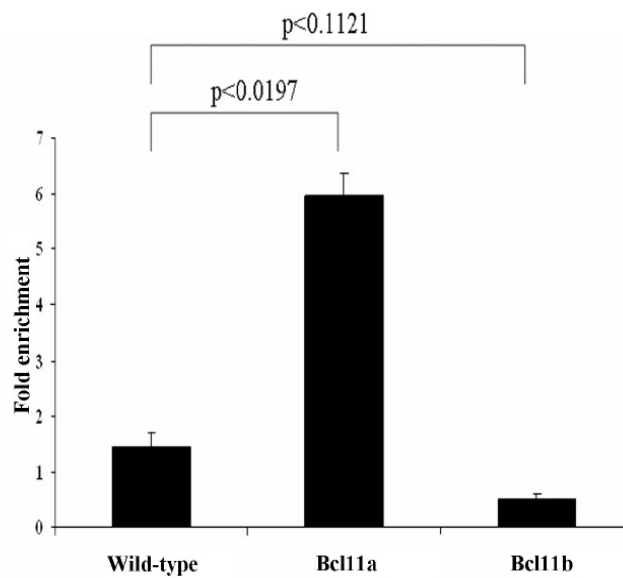Differentiated luminal cells
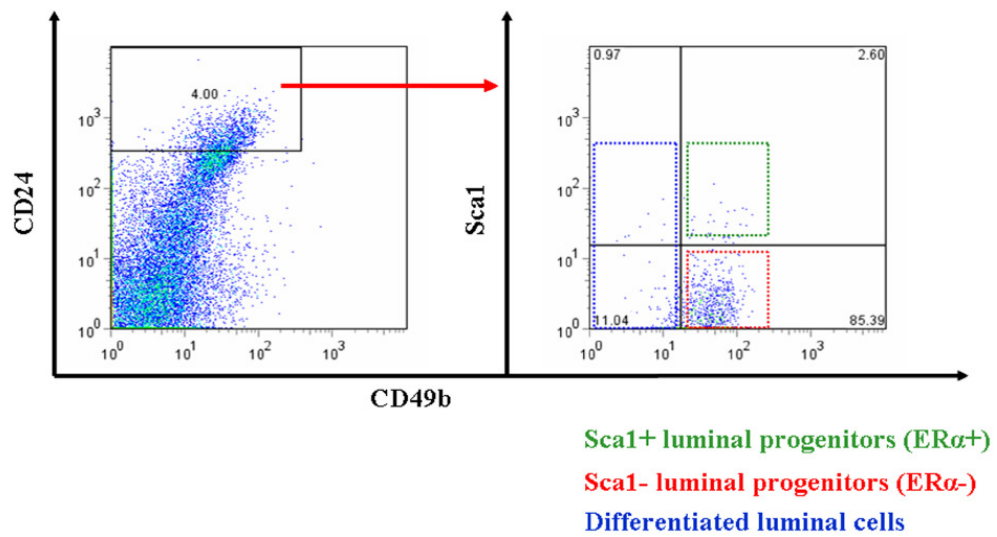
D

Figure 4.19. FACS-gal analysis of *Bcl11*$^{lacZ/+}$ epithelial cells. (A) Distribution of *Bcl11-lacZ* positive (FDG$^+$) mammary epithelial cells in a CD24/CD49f FACS profile. **(B)** Luminal mammary epithelial cells (CD24^{hi}) can be separated into luminal progenitors (CD49b-positive) and differentiated luminal (CD49b-negative) populations. **(C)** Distribution of *Bcl11-lacZ* positive (FDG$^+$) luminal (CD24^{hi}) mammary epithelial cells in a CD49b/Sca1 FACS profile. Analysis shows that *Bcl11a* is expressed in luminal progenitors and in differentiated luminal cells while *Bcl11b* is expressed only in luminal progenitors. **(D)** Graph showing relative enrichment in cloning efficiencies between *Bcl11*$^{lacZ/+}$ FDG-positive and FDG-negative epithelial cells. Error bars denote standard deviation. P values represent student T-test between *Bcl11a/Bcl11b* and wild-type samples (n=2).

173

4.2.7.2 Characterization of $Bcl11^{lacZ/+}$ hematopoietic cells

Both *Bcl11* genes have been shown to be essential for lymphocyte development (Liu et al., ; Wakabayashi et al., 2003b); however the expression of these two genes in other hematopoietic cells was not characterized in detail. Therefore, I performed flow cytometric analysis in combination with FDG staining to determine the expression patterns of *Bcl11* genes in different hematopoietic cells.

The cells of the immune system originate in the bone marrow (BM) where most of them also mature. They then migrate to guard the peripheral tissues, circulate in the blood and in specialized system of vessels called the lymphatic system. All the cellular components of blood and the immune system are derived from the hematopoietic stem cells (HSCs). The pluripotent HSCs are capable of self-renewal and can also differentiate into all the lineages of the blood cells to replenish cells that are damaged or are lost by attrition. HSCs are usually quiescent within the stem cell niche in the BM until they are mobilized from the niche to undergo proliferation and differentiation to generate cells of the immune system. HSCs are identified by their lack of lineage markers (Lin$^-$) and expression of Sca1 (Ly6A/E) and c-kit (CD117) markers (Lin$^-$Sca1$^+$ckit$^+$, KLS) (Spangrude et al., 1988). BM cells were harvested from $Bcl11a^{lacZ/+}$ and $Bcl11b^{lacZ/+}$ adult mice and lineage depleted as described in Chapter 2.10.1. After staining with antibodies to Sca1 and c-kit, cells were incubated with FDG before analysis with flow cytometry. As shown in Figure 4.20A, the percentage of KLS population in the BM of $Bcl11a^{lacZ/+}$ heterozygous mice was ~50% of that compared to the wild-type littermate control (n=3). This indicated that loss of one copy of *Bcl11a* allele resulted in a decrease in the percentage of KLS HSCs, suggesting that *Bcl11a* is a dosage-sensitive gene. About 85% of the KLS cells expressed *Bcl11a*, suggesting the *Bcl11a* was expressed in HSCs and/or MPPs (Figure 4.20B). In contrast, expression of *Bcl11b* in KLS cells was not detected. Most, if not all long term multi-lineage HSC activities reside within this minor KLS fraction of the murine BM. It has been noted that though this fraction is enriched for HSC activity when compared to whole BM, only ~1/30 of KLS cells are actually long-term reconstituting HSCs while the vast majority are multi-potent progenitors (MPPs) (Bryder et al., 2006). Taken together, *Bcl11a* is expressed in HSCs and/or MPPs, and loss of one

Bcl11a allele results in decreased numbers of KLS cells, indicating the importance of *Bcl11a* in maintenance of KLS cells.

HSCs can proliferate and divide to generate MPPs and progenitors with more limited potential such as the megakaryocyte/erythroid progenitors (MEPs), lymphoid-primed multi-potent progenitors (LMPPs), common myeloid progenitors (CMPs) and common lymphoid progenitors (CLPs). These progenitors then proliferate and differentiate to generate the entire hematopoietic lineages. The CMP is the precursor of granulocytes, monocytes/macrophages, eosinophils, neutrophils, dendritic cells and mast cells of the immune system.
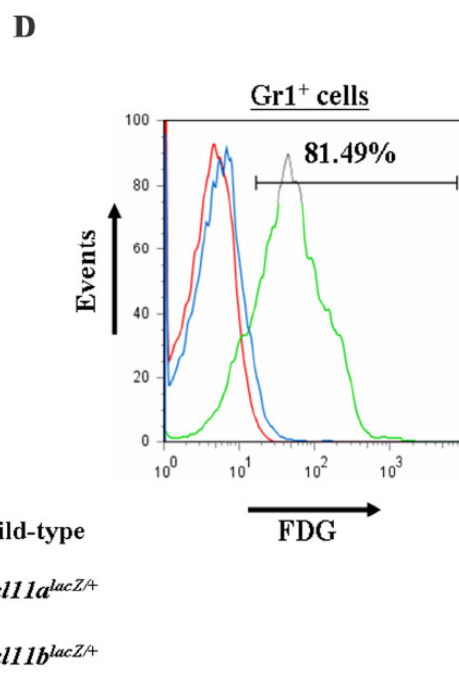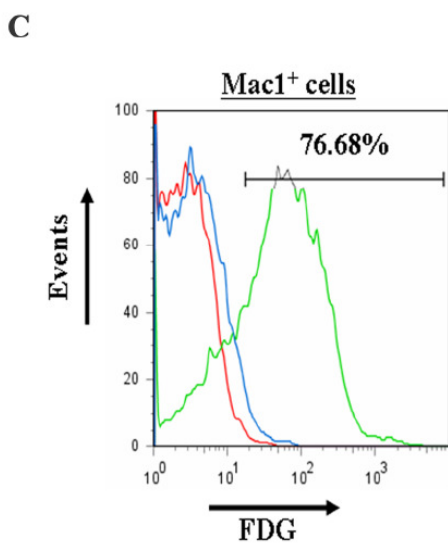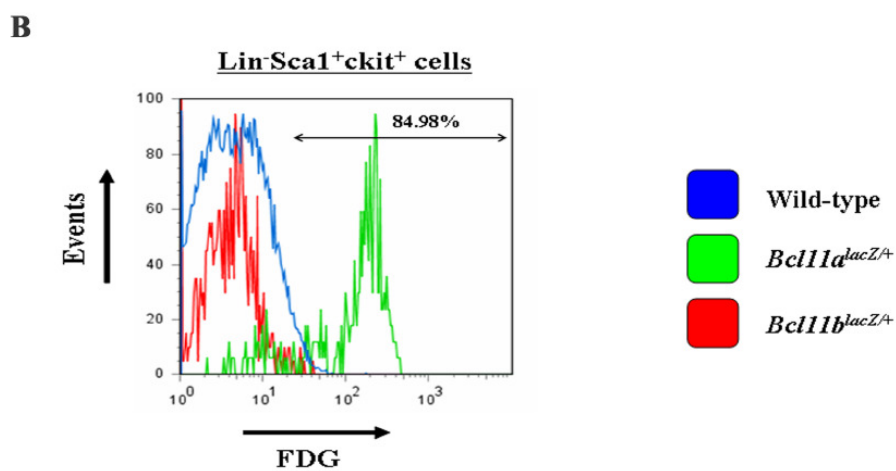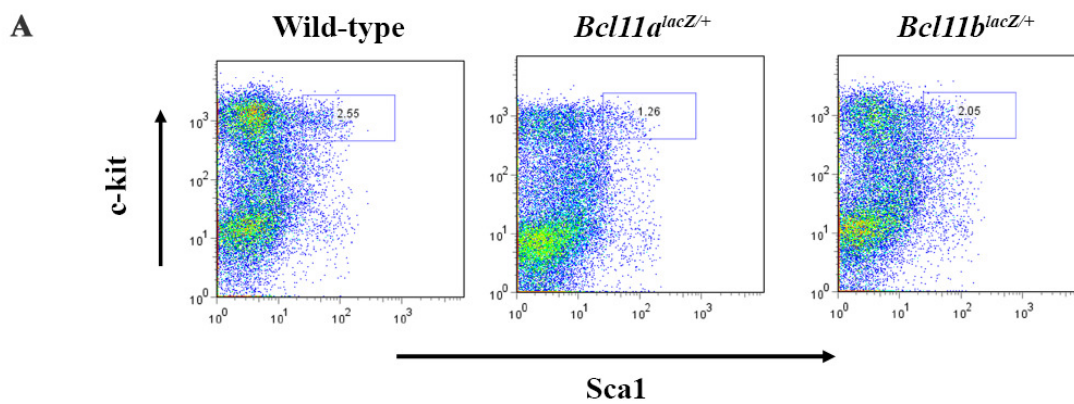
Expression of *Bcl11* genes was determined in the myeloid lineages using antibodies to Mac-1 (CD11b) and Gr-1 (Ly-6G and Ly-6C). Mac-1 is expressed on the surface of activated lymphocytes, monocytes, granulocytes and a subset of NK cells while Gr-1 is a myeloid differentiation marker and expression correlates with granulocyte differentiation and maturation. BM cells were harvested from $Bcl11a^{lacZ/+}$ and $Bcl11b^{lacZ/+}$ adult mice and stained with antibodies to Mac-1 (CD11b) and Gr-1 (Ly-6G and Ly-6C) as described in Chapter 2.10.1. After antibody staining, cells were incubated with FDG before analysis with flow cytometry. As shown in Figure 4.20C, about 77% of Gr-1 positive BM cells expressed *Bcl11a* but not *Bcl11b*. In addition, about 82% of Mac-1 positive BM cells expressed *Bcl11a* but not *Bcl11b* (Figure 4.20D). Taken together, these data suggest that *Bcl11a* but not *Bcl11b* is expressed in myeloid cells.

Next, expression of *Bcl11* genes in erythroid cells was determined using anti-TER119 antibody. TER-119 is expressed on erythroid cells from pro-erythroblast through mature erythrocyte stages. BM cells were harvested from $Bcl11a^{lacZ/+}$ and $Bcl11b^{lacZ/+}$ adult mice and stained with antibody to TER-119 as described in Chapter 2.10.1. After antibody staining, cells were incubated with FDG before analysis with flow cytometry. As shown in Figure 4.20E, about 61% of TER-119 positive BM cells expressed *Bcl11a*. Expression of *Bcl11b* in TER-119 positive BM cells was not detected. Interestingly, a quantitative trait locus (QTL) influencing F cell production maps to *BCL11A* in human thalassemia patients (Menzel et al., 2007). These results suggest that *Bcl11a* may play a role in erythroid development.

The CLPs give rise to the B lymphocytes (B cells) and the T lymphocytes (T cells) which are responsible for adaptive immunity. Activated B cells differentiate into plasma cells that secrete antibodies. Expression of *Bcl11* genes in B cells was detected using the B220 marker. The B220 antigen is expressed on all B cells from the Pro-B stage through to the mature B and activated B cell stages, but is decreased on plasma cells and a subset of memory B cells. Again, BM cells were harvested from *Bcl11a*$^{lacZ/+}$ and *Bcl11b*$^{lacZ/+}$ adult mice and stained with anti-B220 antibody as described in Chapter 2.10.1. After antibody staining, cells were incubated with FDG before analysis with flow cytometry. There was a 50% reduction in B220 positive cells in the BM of the *Bcl11a*$^{lacZ/+}$ heterozygous mice (Figure 4.20F). This indicated that B cells are sensitive to the levels of *Bcl11a* within the cells and that *Bcl11a* is a dosage sensitive gene. Expression of *Bcl11a* was detected in about 86% of B220 positive BM cells while expression of *Bcl11b* was not detected (Figure 4.20G).

In summary, expression of *Bcl11a* was detected in HSCs, myeloid, erythroid and B lymphocytes in the BM. In contrast, expression of *Bcl11b* was negligible in these lineages. Next, expression patterns of *Bcl11* genes in T lymphocytes were determined. Thymocytes were harvested from the thymus of *Bcl11a*$^{lacZ/+}$ and *Bcl11b*$^{lacZ/+}$ adult mice and stained with different T cell markers as described in Chapter 2.10.1. After antibody staining, cells were incubated with FDG before analysis with flow cytometry. Expression of *Bcl11* genes in T cell lineages was first determined using CD4 and CD8 cell surface markers. Expression of *Bcl11a* was only detected in about 3.45% of double-negative thymocytes (DN; CD4$^-$CD8$^-$) and virtually undetected in other T cell lineages (Figure 4.21A). Further analysis of the DN thymocytes using CD44 and CD25 showed that expression of *Bcl11a* was detected only at the DN1 stage (Figure 4.21B). In contrast, expression of *Bcl11b* was detected in all mature single-positive CD4$^+$ or CD8$^+$ T cells, double-positive CD4$^+$CD8$^+$ T cells and in 44.32% of DN T cells (Figure 4.21C). Analysis of the DN thymocytes revealed that *Bcl11b* was expressed in about 24.3% of CD44$^+$CD25$^-$ thymocytes at DN1 stage (Figure 4.21D). As these thymocytes mature, expression of *Bcl11b* was drastically increased and detected in more than 80% of all DN thymocytes from DN2 to DN4 stages (Figure 4.21D). Taken together, these results show that *Bcl11a* is expressed in early DN immature thymocytes at the DN1 stage. As levels of

Bcl11b increase from DN1 stage onwards, expression of *Bcl11a* is down-regulated and only *Bcl11b* is expressed in the T cell lineages (Figure 4.21E). This reciprocal expression of *Bcl11a* and *Bcl11b* during T cell development reflects their unique and potentially antagonistic function: *Bcl11a* might in general suppress T cell development while *Bcl11b* might promote T cell development. Taken together, these results suggest that *Bcl11b* may be critical in regulating T cell fate decision. Indeed, it has been suggested that *Bcl11b* is the key transcription factor that determine T cell fate (Rothenberg, 2007b).

A

Wild-type   *Bcl11a^{lacZ/+}*   *Bcl11b^{lacZ/+}*

c-kit

2.55   1.26   2.05

Sca1

B

Lin⁻Sca1⁺ckit⁺ cells

84.98%

Events

FDG

■ Wild-type
■ *Bcl11a^{lacZ/+}*
■ *Bcl11b^{lacZ/+}*

C

Mac1⁺ cells

76.68%

Events

FDG

D

Gr1⁺ cells

81.49%

Events

FDG

■ Wild-type
■ *Bcl11a^{lacZ/+}*
■ *Bcl11b^{lacZ/+}*
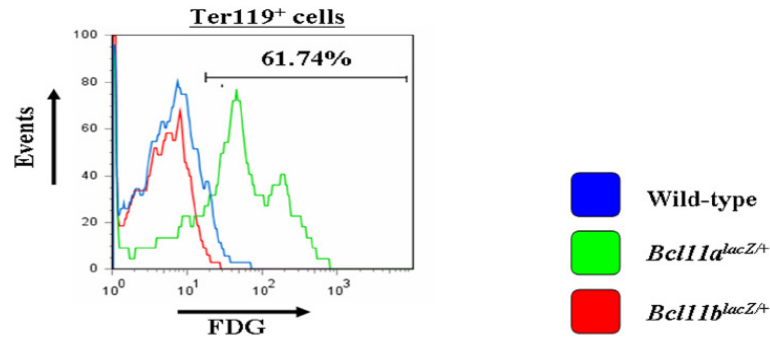
Figure 4.20. FACS-gal analysis of $Bcl11^{lacZ/+}$ bone marrow cells. (A) Flow cytometric analysis of hematopoietic cells shows that there is a decrease in the percentage of lineage-negative Sca1 and c-kit double-positive (KLS) hematopoietic stem cell population in $Bcl11a^{lacZ/+}$ bone marrow. **(B)** FACS-gal analysis shows that 84.98% of KLS cells express $Bcl11a$, suggesting that $Bcl11a$ but not $Bcl11b$ is expressed in 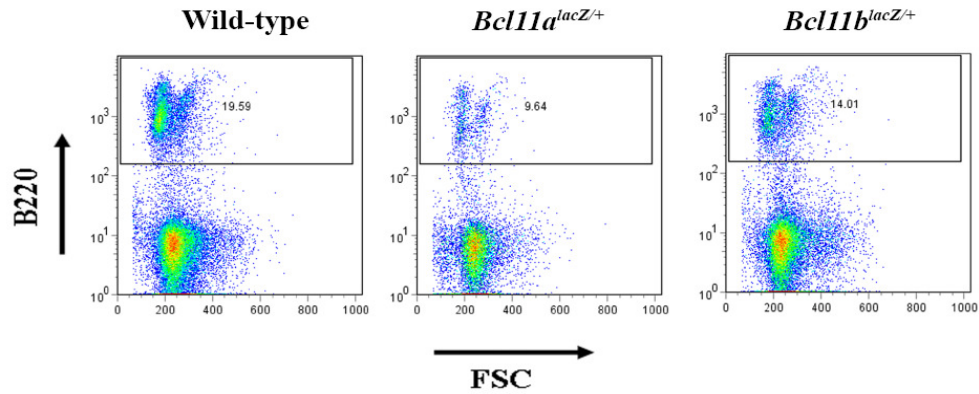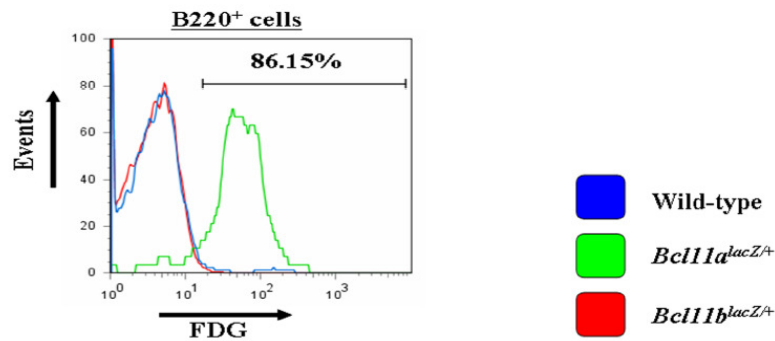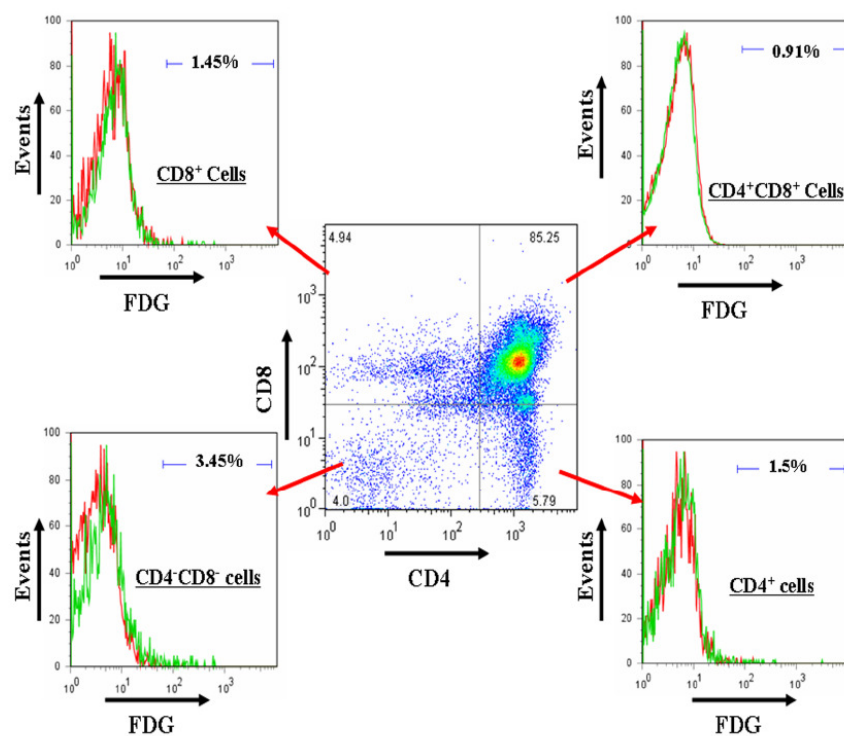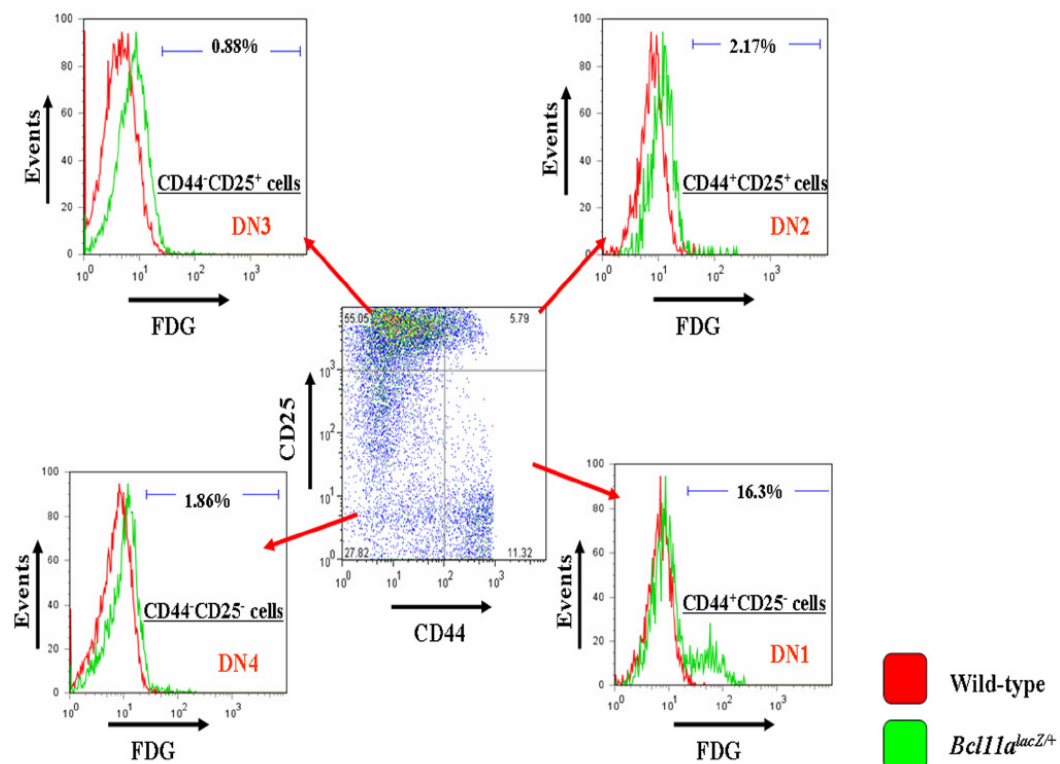KLS hematopoietic stem cells. FACS-gal analysis shows that $Bcl11a$ but not $Bcl11b$ is expressed in **(C)** Mac1-positive macrophages (76.68%), **(D)** Gr1-positive granulocytes (81.49%) and **(E)** TER119-positive red blood cells (61.74%). (%) indicates the % of Gr1/Mac1/TER119 positive cells that express $Bcl11a$. **(F)** Flow cytometric analysis of bone marrow cells also shows that there is about 50% reduction in B220-positive population (B cells) in $Bcl11a^{lacZ/+}$ bone marrow. **(G)** FACS-gal analysis shows that 86.15% of B220-positive cells express $Bcl11a$, indicating that $Bcl11a$ but not $Bcl11b$ is expressed in B cells.

179

Bcl11a^{lacZ/+} **Thymocytes**

A

CD8+ Cells — 1.45%
FDG / Events

CD4+CD8+ Cells — 0.91%
FDG / Events

CD4-CD8- cells — 3.45%
FDG / Events

CD4+ cells — 1.5%
FDG / Events

4.94   85.25
4.0   5.79
CD8 / CD4

B

CD44-CD25+ cells — 0.88% — DN3
FDG / Events

CD44+CD25+ cells — 2.17% — DN2
FDG / Events

CD44-CD25- cells — 1.86% — DN4
FDG / Events

CD44+CD25- cells — 16.3% — DN1
FDG / Events

55.05   5.79
27.82   11.32
CD25 / CD44

Wild-type
Bcl11a^{lacZ/+}

180

Bcl11b^lacZ/+ Thymocytes

C

CD8^+ Cells — 88.13%

CD4^+CD8^+ Cells — 89.13%

CD4^-CD8^- cells — 44.32%

CD4^+ cells — 99.24%

D

CD44^-CD25^+ cells — DN3 — 81.58%

CD44^+CD25^+ cells — DN2 — 86.89%

CD44^-CD25^- cells — DN4 — 85.24%
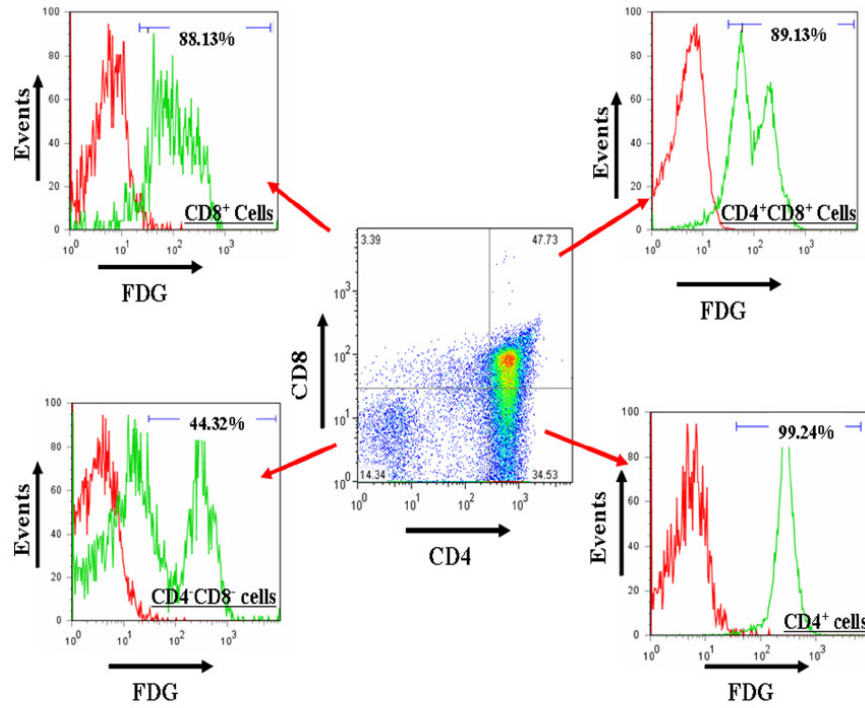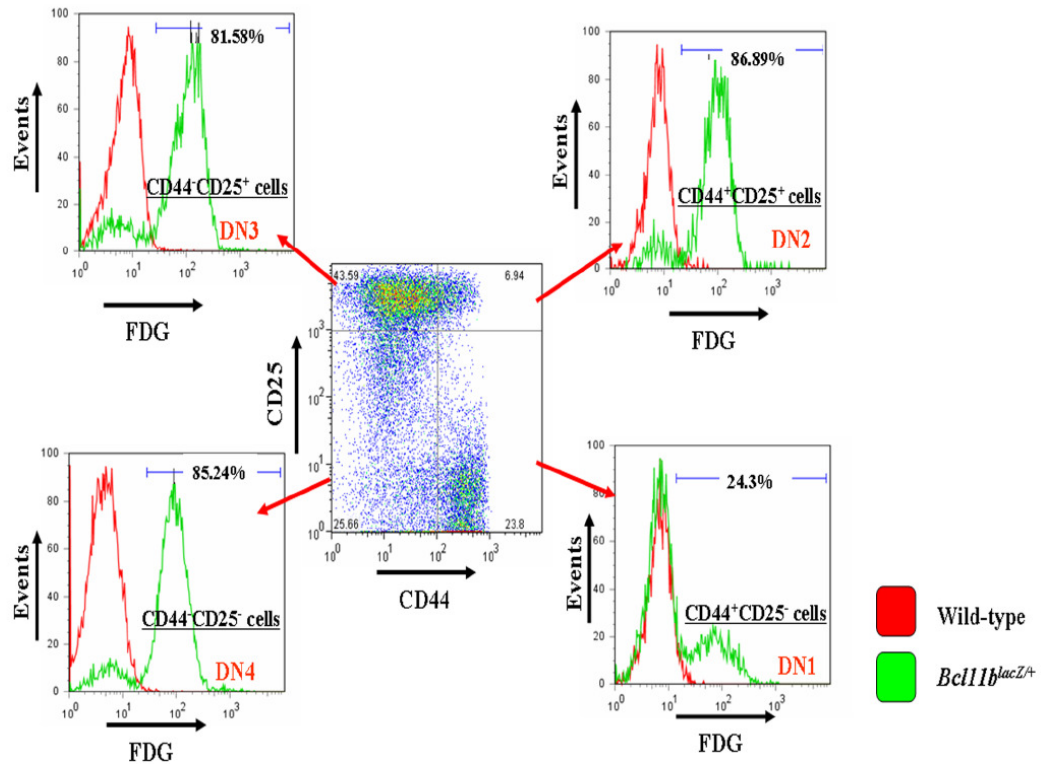
CD44^+CD25^- cells — DN1 — 24.3%
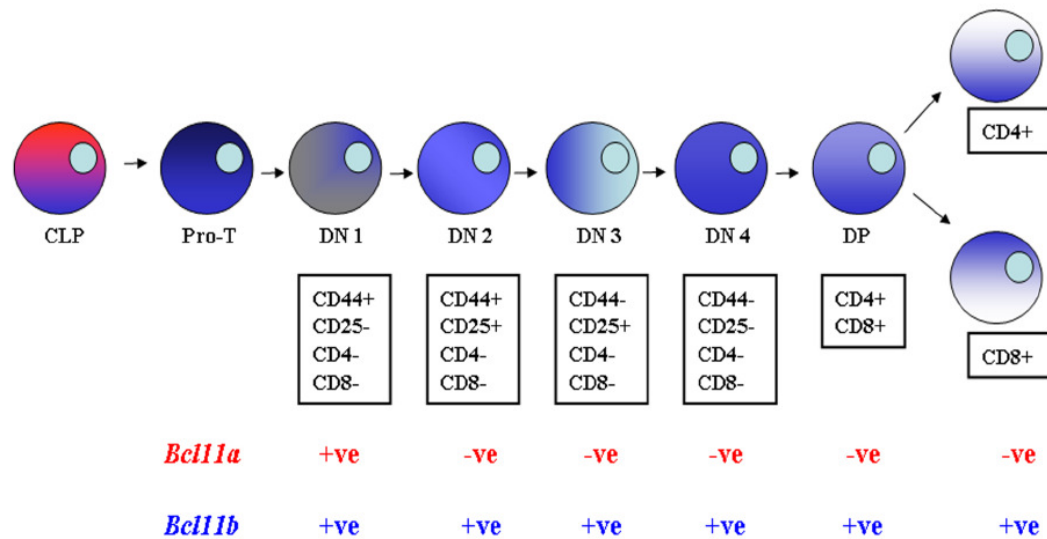
Wild-type
Bcl11b^lacZ/+

181

E

Figure 4.21. FACS-gal analysis of *Bcl11*$^{lacZ/+}$ thymocytes. (A) FACS-gal analysis of *Bcl11a*$^{lacZ/+}$ thymocytes shows that *Bcl11a* is expressed only in a small percentage of CD4 and CD8 double negative thymocytes (3.45%). **(B)** Further analysis of these CD4 and CD8 double negative thymocytes shows that expression of *Bcl11a* is only detected in the CD44$^+$CD25$^-$ (DN1) thymocytes (16.3% of CD44$^+$CD25$^-$ thymocytes express *Bcl11a*). **(C)** In contrast, expression of *Bcl11b* is detected in all thymocytes. About 45% of CD4 and CD8 double negative thymocytes express *Bcl11b*. **(D)** Analysis of the CD4 and CD8 double negative thymocytes shows that *Bcl11b* is expressed from DN1 stage (24.3% of CD44$^+$CD25$^-$ thymocytes express *Bcl11b*) and the expression is maintained throughout T cell development stages. **(E)** Summary of expression of *Bcl11* genes in T cell developmental stages. +ve: expression; -ve: no expression.

4.3   Discussion

In this Chapter, I showed that the new gene targeting system and strategy that our lab had developed as described in Chapter 1 worked efficiently in generating *lacZ*-tagged reporter mice. X-gal staining patterns of *Bcl11*$^{lacZ/+}$ embryos faithfully recapitulated the endogenous *Bcl11* expression. Using whole mount X-gal staining, the spatial and temporal expression patterns of both *Bcl11a* and *Bcl11b* were determined. In addition, the expression of both genes in hematopoietic and mammary epithelial cells was also characterized at a cellular level using FDG staining and flow cytometry. *Bcl11* genes exhibited unique and dynamic expression patterns throughout the developmental time points studied.

4.3.1   Summary of embryonic expression patterns

Analysis of X-gal staining patterns of *Bcl11*$^{lacZ/+}$ embryos showed that both genes were expressed from 10.5 dpc. Expression of neither gene was detected at earlier stages. Some anatomical regions showed overlapping expression of both genes which was maintained throughout embryonic development; while other regions displayed reciprocal expression of the two genes. The primary regions of overlapping expression were in the brain and the craniofacial mesenchyme. Expression of *Bcl11* genes were first detected in the forebrain and in the derivatives of the pharyngeal arches from 10.5 dpc. At 12.5 dpc, expression of both genes became more restricted to regions of the developing brain and to the facial mesenchyme. This expression pattern was maintained at 14.5 dpc. Overlapping expression patterns within these regions suggest that functions of *Bcl11a* and *Bcl11b* might be needed in the development of brain and facial mesenchyme.

Differential expression patterns of *Bcl11* genes were detected outside of the brain and facial mesenchyme. Limb development occurs early in embryonic stages where the reciprocal interaction between the mesenchymal and the ectodermal cells is critical to create the limb buds (Johnson and Tabin, 1997). Expression of *Bcl11a* in the limb buds was detected from 10.5 dpc and its expression was maintained throughout later stages of limb development. In addition, expression of *Bcl11a* was also detected in the developing cartilage and bone. Nevertheless, no apparent abnormalities were observed in *Bcl11a* homozygous mutant embryos at 18.5 dpc. These observations suggest that *Bcl11a* might

not have a major role in the specification of limb fate or a compensatory mechanism exists for the loss of *Bcl11a*. Therefore, further studies are required to address whether *Bcl11a* plays a minor role in limb and/or skeletal development.

Expression of *Bcl11* genes was differentially regulated in the lungs during embryonic development (14.5–18.5 dpc). Transient expression of *Bcl11b* was detected in the lungs. It was expressed at 14.5 dpc and not at 18.5 dpc. In contrast, expression of *Bcl11a* in the lungs started from 18.5 dpc. Mouse lung bud formation occurs early at 9.5 dpc from the laryngotracheal groove and involves mesenchymal-epithelial cell interactions (Costa et al., 2001). During mouse lung development, the pseudoglandular stage (9.5-16.6 dpc) is characterized by formation of the bronchial and respiratory bronchiole tree, which is lined with undifferentiated epithelial cells juxtaposed to the splanchnic mesoderm. There is extensive branching of the distal epithelium and mesenchyme during the canalicular stage (16-17 dpc), resulting in formation of terminal sacs lined with epithelial cells integrating with the mesoderm-derived vasculature. The terminal sac stage [17.5 dpc to postnatal day 5] of lung development is characterized by a coordinated increase in terminal sac formation and vasculogenesis in conjunction with the differentiation of alveolar epithelial type I and II cells. The dynamic expression patterns of *Bcl11a* and *Bcl11b* during embryonic lung development suggest that each of these genes may be involved in different phases of lung development. *Bcl11b* may be involved in the pseudoglandular stage (initial generation of lung structures), while *Bcl11a* may be involved in the terminal sac stage (terminal differentiation of lung alveolar). Future studies could be carried out to determine the precise roles of these transcription factors in lung development.

In addition to the lung, differential expression patterns were also observed in the fetal liver, thymus and mammary gland. The murine fetal liver is organ of intense, but transient site of hematopoietic activity during mid-gestation. It is the initial site of hematopoiesis where hematopoietic cells are generated. T cell progenitors then exit the fetal liver and home to the thymus where the immature thymocytes undergo maturation. Expression of *Bcl11a* in the fetal liver and *Bcl11b* in the thymus was detected in early embryonic development. *Bcl11b* was detected in the developing thymus at 14.5 dpc, a time at which most thymocytes are T cell precursors, and its expression was maintained

at 18.5 dpc. These results together with the knockout phenotypes (Liu et al., ; Wakabayashi et al., 2003b) demonstrate that *Bcl11* genes are essential for the hematopoietic lineages.

4.3.2 Differential *Bcl11* expression patterns in hematopoietic lineages

Expression of *Bcl11a* and *Bcl11b* was studied in bone marrow hematopoietic cells using FDG staining. In addition to its known expression and function in B cells, expression of *Bcl11a* was also detected in KLS HSCs and/or multi-potent progenitors, myeloid cells and red blood cells; suggesting that *Bcl11a* may also play role(s) in these hematopoietic lineages. Recently, a quantitative trait locus (QTL) influencing F cell production mapping to *BCL11A* in human thalassemia patients has been identified (Menzel et al., 2007). In addition, *Bcl11a* is a dosage-sensitive gene where loss of one allele resulted in reduction in numbers of B cells and KLS HSCs (Figure 4.18A and 4.18F). These, together with some of my work which showed that deletion of *Bcl11a* in adult hematopoietic cells resulted in the initial expansion, followed by depletion of the KLS population (personal observations), suggest that *Bcl11a* plays an important role in maintenance of the hematopoietic lineages.

In the adult thymus, expression of *Bcl11a* was only detected in a small percentage of thymocytes. Using different molecular markers, I found that *Bcl11a* expression was only detected in 16.3% of DN1 immature thymocytes and not in mature T cells. In contrast, expression of *Bcl11b* was detected only in T cell lineages and its expression was detected at all stages of T cell development. *Bcl11b* expression was detected from DN1 immature thymocyte stage and was drastically up-regulated from the DN2 stage, a critical stage in T cell linage commitment. This expression pattern thus supports the proposal that *Bcl11b* is the main T cell lineage determinant in thymocyte development (Rothenberg, 2007a). The dynamic reciprocal expression patterns of *Bcl11* genes in immature thymocytes suggest that the interplay between the levels of these genes in hematopoietic progenitors may be critical for lymphocyte development.

4.3.3 Dynamic differential expression patterns in mammary lineages

Recent studies have shown that transcription factors that normally play critical roles in T helper cell lineage determination are also essential for mammary lineage determination (Asselin-Labat et al., 2007; Khaled et al., 2007; Kouros-Mehr et al., 2006). This complements the existing paradigm that mammary development and cell fate decisions are determined by steroids and prolactin (Hennighausen and Robinson, 2005). Because *Bcl11* genes are expressed in a dynamic and contrasting pattern in hematopoietic cells and they are a pair of transcription factors that have been shown to be essential for B and T cell determination from a common lymphoid progenitor, I hypothesized that *Bcl11* genes also play important roles in mammary cell fate determination. Using the *Bcl11-lacZ* reporter mice, I found that *Bcl11* genes were among the earliest known genes to be expressed specifically in the mammary gland. Expression of *Bcl11b* was detected from 10.5 dpc in the milk line and from 12.5 dpc, its expression was detected within the mammary buds. In contrast, expression of *Bcl11a* within mammary buds was detected only from 13.5 dpc.

These differential expression patterns were maintained during postnatal mammary development where *Bcl11a* was expressed in both cap and body cells of the TEBs and *Bcl11b* was detected only in the neck region of TEBs in the cap cell layer. Consistent with these observations, *Bcl11a* was found to be expressed in both the luminal and basal layers of the mature virgin duct while expression of *Bcl11b* was detected predominantly in the basal layer. This was confirmed by both semi-quantitative and quantitative PCR using FACS sorted luminal and basal fractions. Interestingly, up-regulation of both genes was detected at early gestation. *Bcl11a* was detected in luminal layers of ducts and in differentiating alveoli. In contrast, expression of *Bcl11b* remained primarily in the basal layer of ducts and was not detected in the differentiating alveoli. This reciprocal expression pattern was maintained throughout gestation. During lactation, only expression of *Bcl11a* was detected in the differentiated luminal secretory cells. Further analysis using cell surface markers and flow cytometry showed that *Bcl11a* was expressed in luminal progenitors and their differentiated derivatives while only a small percentage of luminal progenitors expressed *Bcl11b*. In addition, a 6-fold enrichment in cloning efficiencies of *Bcl11a*-expressing epithelial cells which further confirmed that

many luminal progenitors expressed *Bcl11a*. These results suggest that *Bcl11a* may be important for differentiation of the luminal lineages while *Bcl11b* may be important for maintaining basal cell identity and/or suppressing luminal cell fate. During involution, there was a dramatic up-regulation of *Bcl11b* levels 24 hours after initiation of involution, followed by a sharp decline before peaking again at 96 hours involution time point. On the other hand, levels of *Bcl11a* increased gradually during involution and peaked at 72 hours involution. Thus *Bcl11* genes may play different roles during the involution phase. While *Bcl11b* may be important for the first phase of involution, expression pattern of *Bcl11a* suggests that it may play an important role during the second phase of involution. Taken together, the unique and dynamic expression patterns of *Bcl11* genes during mammary gland development suggest that these two genes play important roles in the mammary gland. The expression data also laid a solid ground for the characterization of the mammary phenotypes as described in Chapters 5 and 6.

In summary, I have detailed the spatial expression patterns of *Bcl11* genes during embryonic and adult development using the *Bcl11^{lacZ/+}* mice that I have generated. X-gal staining patterns reveal that the brain and craniofacial mesenchyme are the two main regions of overlapping expression. Differential expression of the two genes was detected in the developing limbs, cartilage/bone, lung, hematopoietic lineages and mammary gland. Dynamic expression patterns of *Bcl11* genes during mammary gland development were observed and their expression in different epithelial populations suggests that they have roles in mammary lineage commitment. These results, together with a recent study that identified mutations in *BCL11A* in human breast cancer (Wood et al., 2007) prompted me to investigate the roles of *Bcl11* genes in mammary gland development. Based on these observations, I hypothesized that *Bcl11a* may be essential for luminal cell differentiation while *Bcl11b* may be important for maintaining basal identity and/or suppressing luminal cell fate. In Chapter 5, I will describe characterization of the functions of *Bcl11* genes in mammary development in the embryo and postnatal virgin glands.